

1-1-1965

Control rod calibrations of a coupled core reactor

Richard Lee Jaworski
Iowa State University

Follow this and additional works at: <https://lib.dr.iastate.edu/rtd>

 Part of the [Engineering Commons](#)

Recommended Citation

Jaworski, Richard Lee, "Control rod calibrations of a coupled core reactor" (1965). *Retrospective Theses and Dissertations*. 18349.
<https://lib.dr.iastate.edu/rtd/18349>

This Thesis is brought to you for free and open access by the Iowa State University Capstones, Theses and Dissertations at Iowa State University Digital Repository. It has been accepted for inclusion in Retrospective Theses and Dissertations by an authorized administrator of Iowa State University Digital Repository. For more information, please contact digirep@iastate.edu.

CONTROL ROD CALIBRATIONS
OF A
COUPLED CORE REACTOR

by

Richard Lee Jaworski

A Thesis Submitted to the
Graduate Faculty in Partial Fulfillment of
The Requirements for the Degree of
MASTER OF SCIENCE

Major Subject: Nuclear Engineering

Signatures have been redacted for privacy

Iowa State University
of Science and Technology
Ames, Iowa

1965

TABLE OF CONTENTS

	Page
INTRODUCTION	1
LITERATURE SURVEY	3
REACTOR KINETIC EQUATIONS	6
One Slab Core Kinetic Equations	6
Two Slab Core Kinetic Equations	13
DESCRIPTION OF THE UTR-10 CORE AND CONTROL RODS	33
EXPERIMENTAL PROCEDURES AND RESULTS	36
Positive Period Measurements - One Slab	36
Rod Drop Method - One Slab	38
Positive Period Measurements - Two Slabs	44
Rod Drop Method - Two Slabs	51
COMPARISONS AND CONCLUSIONS	53
SUGGESTIONS FOR FURTHER STUDY	59
LITERATURE CITED	60
ACKNOWLEDGMENTS	62
APPENDIX A	63
Computer Solutions and Flow Sheets	63
Negative Insertions into a One Slab Reactor	63
Negative Insertions into a Two Slab Reactor	73b
APPENDIX B	98
Development of the Kinetic Equations for a Two Slab Core	98
APPENDIX C	100
Matrix Derivation	100
APPENDIX D	106
Miscellaneous Tables	106

INTRODUCTION

The time response of a nuclear reactor is often assumed to be described by the spatially independent point reactor kinetics equations (5, 6). These equations are strictly valid only if the spatial distribution of the neutron flux remains in the fundamental mode during the transient. The transient shape of the neutron flux may be affected by spatially localized reactivity disturbances which often occur in large and multi-region reactors. Such shape changes in the spatial distribution can affect measurements of reactivity. Therefore time and spatial dependence must be considered in the study of the transient problem (9).

A two slab core is one which consists of two regions of fuel which separately are subcritical but because of their proximity are critical due to the exchange of neutrons between them. Each serves as an external source of neutrons to the other and the separate regions are coupled in that neutrons born in one slab are capable of inducing fission in the other. Apart from this coupling each region possesses its own localized reactivity, therefore a tilting of flux shape and neutron density become possible. The degree of this tilting increases as the reactivity difference between the two slabs increases. The purpose of this thesis is to describe the behavior of the two semi-independent fuel regions after the introduction of a change in reactivity such as would occur

in a rod calibration experiment and to determine the effect this behavior would have on the measurement of this reactivity. For this purpose, the two slab core system was approximated by two coupled point reactors and the appropriate reactor kinetic equations for such a system were derived and programmed for solution on the IBM 7074 computer. The response of the system to positive and negative step changes in reactivity was obtained. Similar programs were written for the spatially independent point reactor kinetics equations. The results from these programs were used to calibrate the control rods of the UTR-10 reactor at Iowa State University.

LITERATURE SURVEY

The calibration of control rods is one of the important experiments which is performed periodically on a nuclear reactor. Once calibrated, the control rod may serve as a standard for measurement of changes in the reactor core's reactivity. Thus it is possible to ascertain the reactivity worth of changes caused by the addition of experimental materials and equipment to the core or the worth of changes due to variations in temperature and fuel composition. The "rod drop" and "positive period measurements" are the procedures most often used, however other methods such as distributed poisons, rod oscillation, and others are applicable. The sudden insertion of a control rod into a critical reactor is known as a rod drop experiment; removal of a rod from a critical reactor and measurement of the rate of power increase, after transient periods have died away, constitute a positive period measurement. Most analysis of rod calibration data is based on the spatially independent reactor kinetics equations. Avery (1) and Henry and Curlee (7) point out that this spatial independence is not justified when the reactor consists of two distinct fuel regions. Baldwin (2) and Danofsky (4) suggest that a model based upon a two point reactor is a better description of the system. Baldwin (2) made an analytical study of the kinetics of the Argonaut reactor which has two separate fuel regions

also called slabs. By applying the diffusion equation to each slab independently, and justifying separability of time and space variables by noting that the reactor showed a single stable period, expressions were derived which involved a slab interaction term. These expressions explained the phenomenon of flux tilting and demonstrated the need of knowing the amplitude of the average flux in each as well as the period when determining the worth of a control rod by positive period measurement. He notes that measurements based upon techniques in which one rod is withdrawn from one slab as the rod in the other slab is inserted are apt to be in error due to the resulting increase in flux tilting. In discussing the rod drop method as applied to a two slab core, a diffusion equation is written for each slab, which assumes the presence of only one group of delayed neutrons. Also it is assumed that the flux level in each slab, shortly after the negative step is made, to be that of a subcritical reactor with a built-in source equal in magnitude to the steady-state delayed neutron source level of the critical system. It is also assumed that this source does not decay and that the interchange time of neutrons travel between slabs can be neglected. The resulting expressions relate the flux in each slab prior to the drop to the flux at the new assumed steady-state level as a function of the reactivity worth of the rod.

This work, with modifications, was carried further as

part of a study made by Danofsky on the kinetic behavior of coupled reactor cores. The two region kinetics equations were based on one group of delayed neutrons and solved for positive periods on an analog computer. These results were similar to those discussed by Baldwin. The effect of flux tilting on control rod worth as measured by positive periods is discussed and an approximation of the flux tilting in the UTR-10 is made by assuming that the excess reactivity of the reactor is evenly divided between the two fuel regions.

REACTOR KINETIC EQUATIONS

In reactors where the fuel is located in one distinct region, the region can be approximated as a point in order to remove the spatially dependent variables of the reactor kinetics equations. Similar point approximations can be applied to multiregion reactor systems to simplify the solution of the time dependent neutron balance equations. Even though the resulting equations are spatially independent, the prediction of the transient behavior is based upon the presence of several spatially distributed sources. This study considers reactors consisting of one and two fuel regions. Each fuel region, also referred to as a fuel slab, is approximated as a point.

One Slab Core Kinetic Equations

The standard inhour equation can be derived from the time dependent neutron balance equations which relate the thermal neutron density and concentration of delayed neutron precursors in a bare homogeneous assembly.

$$\frac{dn}{dt} = \frac{Kn}{\ell} - \frac{n}{\ell} - \frac{K\lambda_{avg}\beta n}{\ell} + \sum_{i=1}^M \lambda_i \gamma_i C_i \quad (1)$$

$$\frac{dC_i}{dt} = -\lambda_i C_i + \frac{K\beta_i n}{\ell} \quad (2)$$

In these equations

$n = n(t)$ = average neutron density as a function of time

K = neutron reproduction number for a finite geometry

ℓ = prompt neutron lifetime

λ_1 = decay constant of the "1"th delayed neutron group

$C_1 = C_1(t)$ = density of the "1"th delayed neutron group precursor

m = number of delayed neutron groups

β_1 = "1"th group fraction of total neutrons from fission

$\beta = \sum_{i=1}^m \beta_i$ = total delayed neutron fraction

γ_1 = effectiveness in producing fissions of the "1"th group of delayed neutrons compared with prompt neutrons

$\gamma_{\text{avg}} = \beta^{-1} \sum_{i=1}^m \gamma_i \beta_i$ = average delayed neutron effectiveness.

Because Equations 1 and 2 are linear and first order, solutions of the form

$$n(t) = n_0 e^{\omega t} \quad (1a)$$

and

$$C_1(t) = C_{10} e^{\omega t} \quad (2a)$$

may be superimposed. In the above equations, n_0 and C_{10} are the values of the thermal neutron concentration and the concentration of the precursor of the "1"th group of delayed neutrons, respectively, at time $t = 0$. Such super position solutions are possible for only certain values of the parameter ω which has the dimensions of reciprocal time. By substituting Equations 1a and 2a into

Equations 1 and 2, respectively, and defining reactivity, ρ , as

$$\rho = \frac{K - 1}{K} = \frac{\delta K}{K},$$

the relationship to satisfy the superposition solution for m groups of delayed neutrons is obtained. This result is the spatially independent kinetic equation

$$\rho = \frac{\omega l}{1 + \omega l} + \frac{1}{1 + \omega l} \sum_{i=1}^m \frac{\gamma_i \beta_i \omega}{\lambda_i + \omega} \quad (3)$$

commonly referred to as the inhour equation. Equation 3 is of degree $m + 1$ and therefore has $m + 1$ distinct roots of ω for each value of reactivity. Figure 1 shows ρ as a function of ω for six groups of delayed neutrons.

Equations 1, 2, 1a, and 2a are used in conjunction with the initial conditions,

$$\frac{dc_1(0)}{dt} = 0, \quad n(t) = n(0)$$

in the derivation of an expression for the neutron density ratio, $n(t)/n(0)$, where $n(t)$ is the neutron density at a time t after a step change in reactivity and $n(0)$ is the steady state neutron density just prior to when the change is made. This expression, as given by Baldwin et al. (3), is

$$\frac{n(t)}{n(0)} = \sum_{j=1}^{m+1} A_j e^{\omega_j t} \quad (4)$$

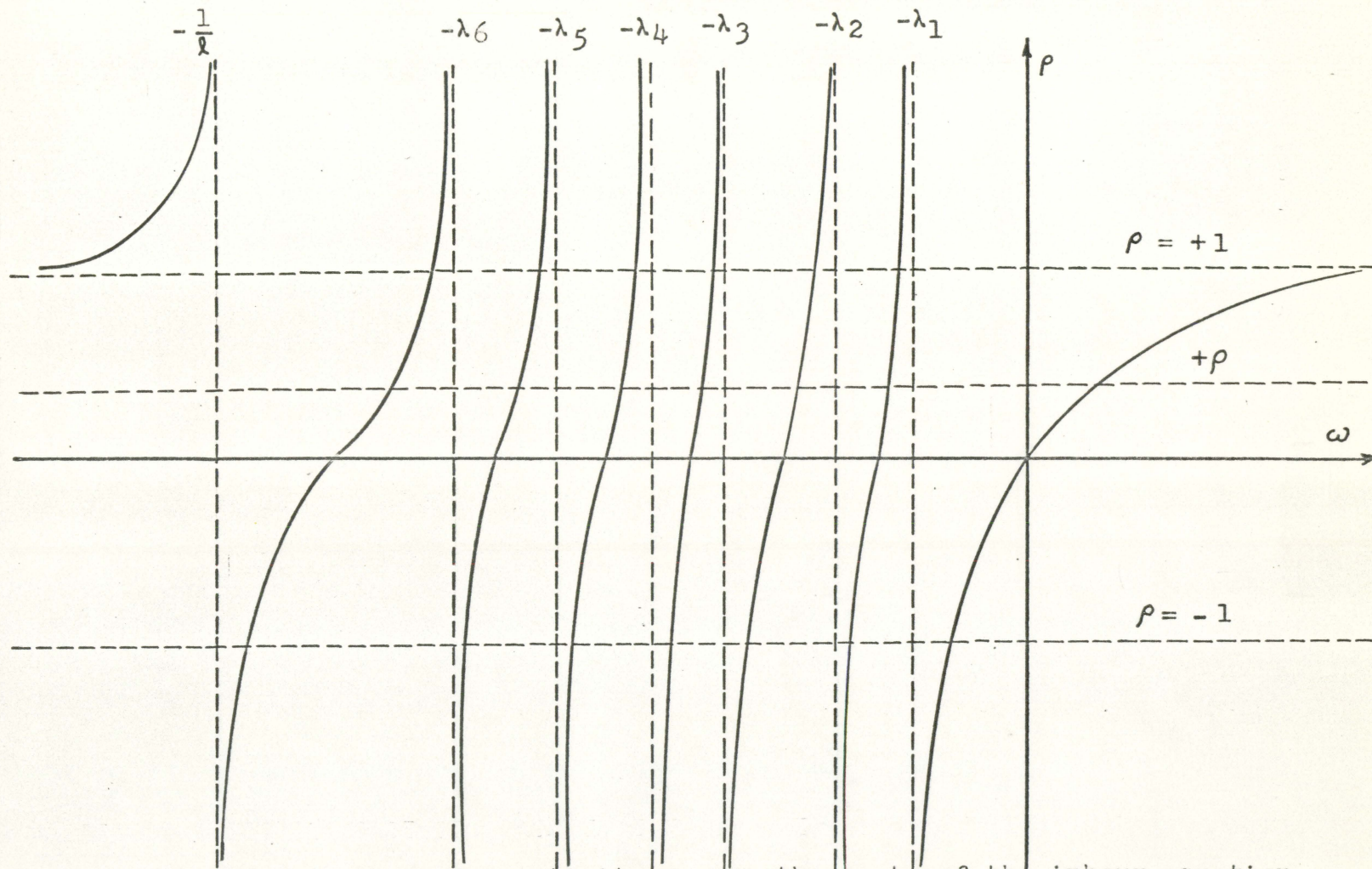


Figure 1. General plot of reactivity versus the roots of the inhour equation for a one slab core

where

$$A_j = (1 - \rho) \frac{\ell + \sum_{i=1}^m \frac{\gamma_i \beta_i}{\omega_j + \lambda_i}}{\ell(1 - \rho) + \sum_{i=1}^m \frac{\gamma_i \beta_i \lambda_i}{(\omega_j + \lambda_i)^2}} \quad (5)$$

Equation 4 is used to evaluate the worth of either a negative or positive step change in reactivity.

Examination of Figure 1 shows that, in the case of a positive step change in reactivity, there is one positive and six negative roots to Equation 3. As a result, all but the first term in the neutron density ratio equation eventually become negligible. When this has happened, the flux is said to be increasing on a stable period, T , which is the reciprocal of the positive ω root. Equation 3 then reduces to

$$\rho = \frac{\ell}{\ell + T} + \frac{T}{\ell + T} \sum_{i=1}^m \frac{\gamma_i \beta_i}{1 + \lambda_i T} \quad (6)$$

A typical curve showing the relationship between reactivity and period is shown in Figure 2.

For a negative step change, seven negative roots must be considered and all terms in the density ratio equation contribute to the total value of the ratio as each term decreases exponentially with time. Figure 3 shows the relationship between flux ratio and reactivity for various values of time after the change is introduced. The control

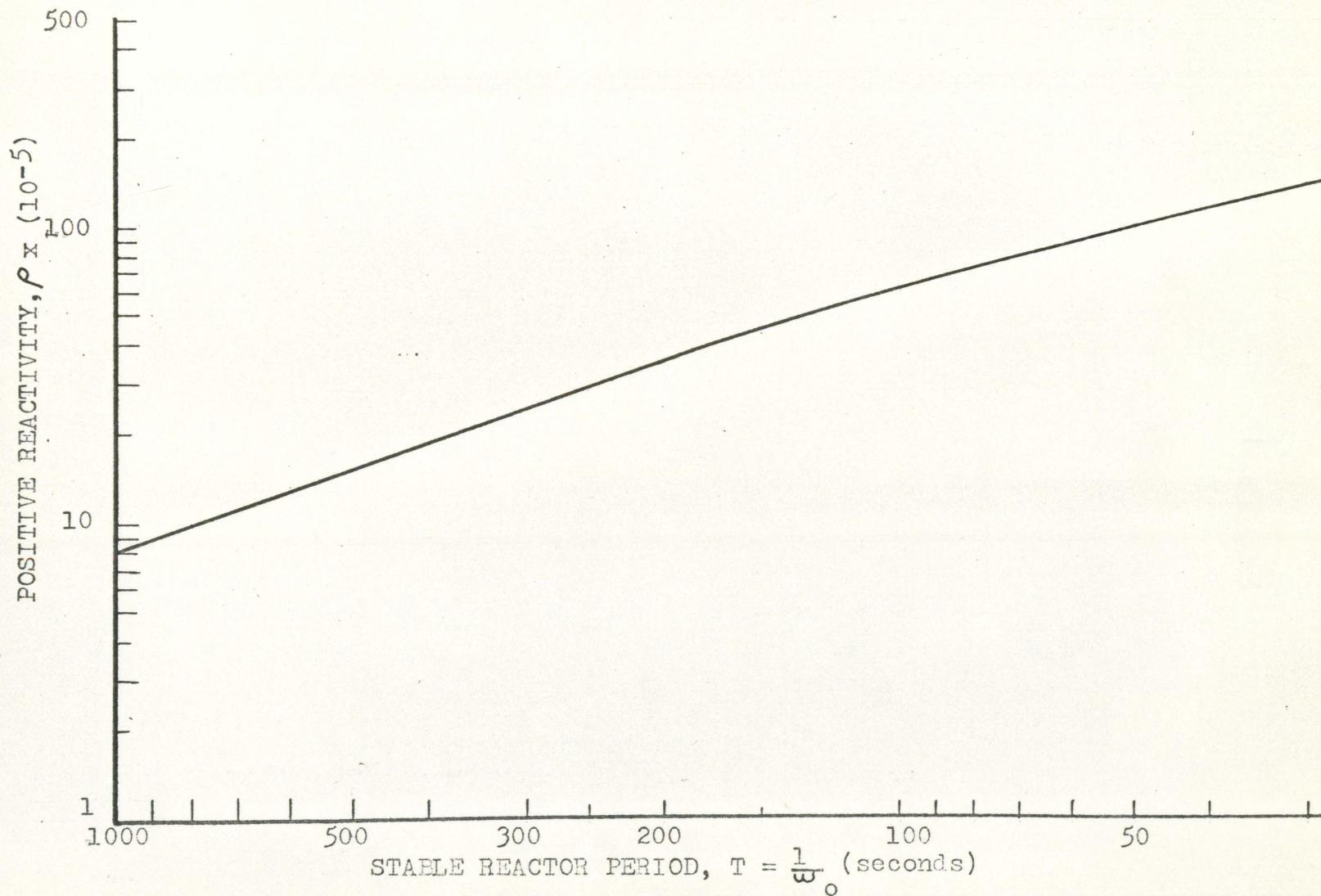


Figure 2. Reactivity versus stable reactor period for a one slab core reactor
 ($\beta = 0.0065$, $\gamma_{avg} = 1.034$, $\lambda = 0.0001$ seconds)

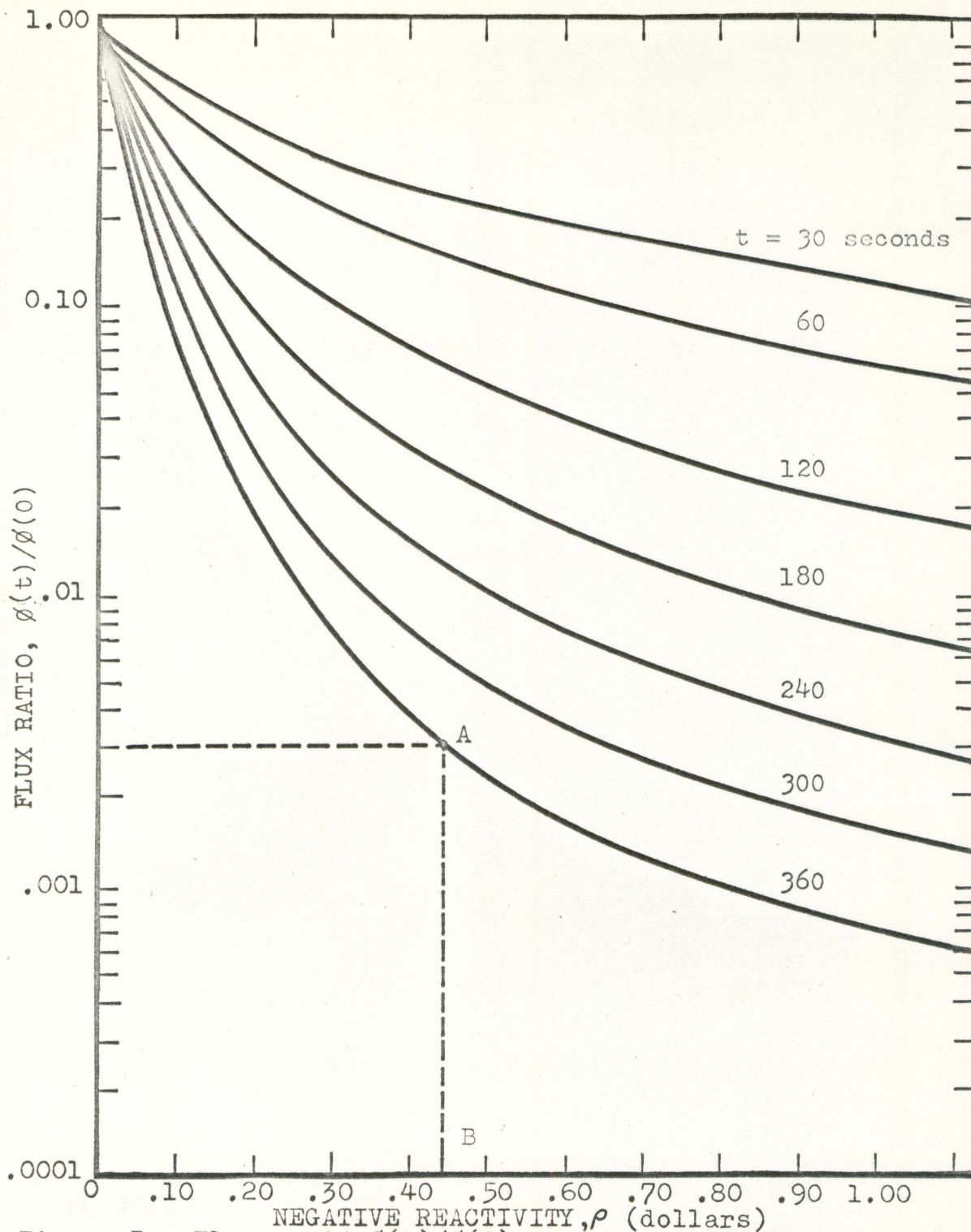


Figure 3. Flux ratio, $\phi(t)/\phi(0)$, versus negative reactivity, ρ , \$ at time, t , seconds after rod drop into one slab core ($\beta = 0.0065$, $\gamma_{\text{avg}} = 1.034$, $\lambda = 0.0001$ seconds)

rod reactivity worth is determined by measuring the flux ratio after the rod is dropped into the critical reactor. The measured density ratio intersects the appropriate time curve, point A, and is then projected onto the abscissa to obtain point B, the corresponding reactivity of the portion of the rod dropped. Ideally, for the same rod drop, all values of $n(t)/n(0)$ should produce the same value of ρ .

The flowsheets of the IBM 7074 code written to numerically evaluate the roots, "A_j" coefficients and the density ratio are presented in Appendix A.

Two Slab Core Kinetic Equations

Figure 4 is a schematic representation of the two slab core considered in this study. Each slab is a subcritical assembly of fuel elements which is made critical by neutron exchange with the opposite slab. The same basic assumptions are made in deriving the kinetic equations for the two slabs as for the one slab except a source term must be added to account for the neutron exchange between slabs. Thus, Equation 1 becomes

$$\frac{dn}{dt} = \frac{Kn}{\ell} - \frac{n}{\ell} - \frac{Kv_{avg}\rho n}{\ell} + \sum_{i=1}^M \nu_i \lambda_i C_i + S(t^*) \quad (7)$$

where $S(t^*)$ represents the source of neutrons from the opposite slab.

The thermal neutron density in each slab would generally

Shim rod

Regulating rod

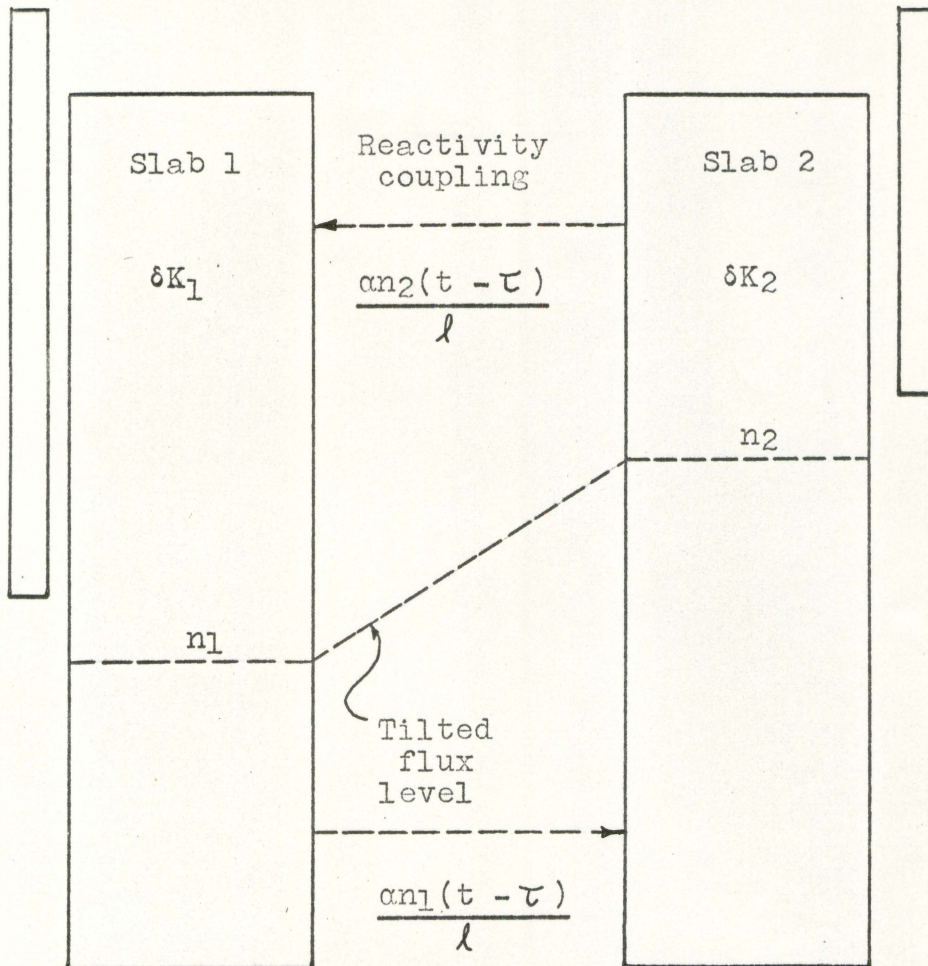


Figure 4. Model of two slab core reactor

be a spatially dependent function but because the source regions are narrow and well reflected, experimental measurements, Baldwin (2), show that there is very little difference between the average thermal neutron density within the slab and the density measured by a detector placed at the slab's edge. Therefore assuming an average value of neutron density has little effect on measurements of rod worth. This assumption is valid only in the fuel regions and does not apply to the internal graphite reflector where the thermal density varies over a greater range.

The intensity of the interaction source term in the above equation is assumed to be proportional to the neutron density in the opposite slab at the time $t - \tau$, where t is the reference time and τ is the time required for a neutron disturbance to travel from one slab to the other. The coupling coefficient, α , is assumed to be the fraction of the average neutron density of the adjacent slab which interact within the slab being described. Thus, Equation 7, as applied to slab 1, becomes

$$\frac{dn_1}{dt} = \frac{K_1 n_1}{\ell} - \frac{n_1}{\ell} - \frac{K_1 v_{avg} \beta n_1}{\ell} + \sum_{i=1}^m v_1 \lambda_i C_{i1} + \frac{\alpha}{\ell} n_2(t - \tau). \quad (8)$$

A similar expression can be written for slab 2 if it is assumed that ℓ , β_1 , and α are the same for both slabs. Examination of the above equation shows that the coupling

term is independent of the neutron density in slab 1. Experiments show that there is a difference between the neutron densities in each slab and "flux tilting" is one result of the semi-independent behavior of the slabs. It is shown in Appendix B that when the above equation is combined with the precursor concentration equation, Equation 2; Equations 1a and 2a; and a similar set of equations describing the other slab, the result is an equivalent inhour expression for a two slab core;

$$\left| \begin{array}{cc} \frac{\delta K_1}{\ell} - \omega - \frac{K_1}{\ell} \sum_{i=1}^m \frac{\gamma_i \beta_i \omega}{\lambda_i + \omega} & \frac{\alpha}{\ell} e^{-\omega \tau} \\ \frac{\alpha}{\ell} e^{-\omega \tau} & \frac{\delta K_2}{\ell} - \omega - \frac{K_2}{\ell} \sum_{i=1}^m \frac{\gamma_i \beta_i \omega}{\lambda_i + \omega} \end{array} \right| = 0 \quad (9)$$

where $\delta K = K - 1$.

The presence of two distinct "K" terms indicates that semi-independent behavior of both slabs is possible. Also it is seen that each slab would follow the general inhour equation if there was no interaction between them. The chief difference between this equation and the standard inhour equation, Equation 3, is that K_1 and K_2 are both functions of ω instead of the simpler one slab K vs. ω relationship as before. Another important difference is that evaluation of the determinant leads to a product of a $2(m + 1)^{th}$ expression

in ω and $e^{-2\omega\tau}$. When the reactor is just critical, $\omega = 0$ and Equation 9 reduces to

$$\delta K_1 = \frac{\alpha^2}{\delta K_2} \quad (10)$$

This critical relationship between δK_1 and δK_2 is shown in Figure 5. Should δK_1 be changed and δK_2 remain constant, the overall system becomes super or subcritical. The amount of change in δK_1 , $\Delta \delta K_1$, is equated to ρ'_1 by the definition

$$\rho'_1 = \frac{\Delta \delta K_1}{\Delta \delta K_1 + 1} = \rho_1 - \rho_\infty \quad (11)$$

where

$$\rho_\infty = \frac{\alpha^2}{\alpha^2 + \delta K_2} \quad (12)$$

If Equation 9 is solved for K_1 and combined with the definitions given above, the result is

$$\rho'_1 = \frac{\alpha^2 e^{-2\omega\tau} + \omega l (\delta K_2 - \omega l) + (\delta K_2 - \omega l K_2 - \omega l - K_2 \omega \Sigma) \omega \Sigma}{\alpha^2 e^{-2\omega\tau} + \omega l (\delta K_2 - \omega l) + \delta K_2 - \omega^2 l K_2 \Sigma - \omega l - K_2 \omega \Sigma} - \rho_\infty \quad (13)$$

where

$$\Sigma = \sum_1^m \frac{\gamma_1 \beta_1}{\lambda_1 + \omega} \quad (14)$$

Figure 6 shows the general shape of the $\rho'_1 - \omega$ curves for a fixed value of δK_2 . These curves have the same general characteristics as those of the simpler inhour equation as shown in Figure 1. In both cases, $\omega = 0$ at $\rho'_1 = 0$ and poles

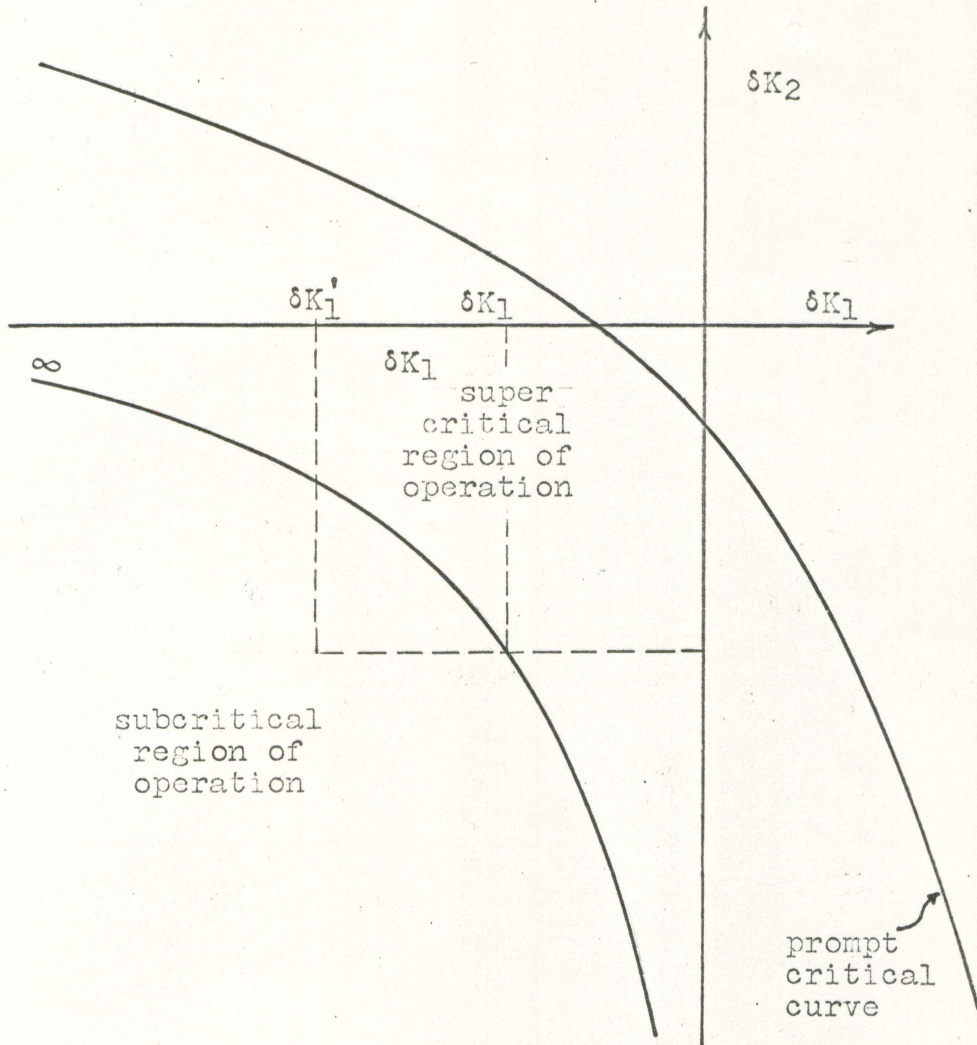


Figure 5. General plot of reactivity of slab one versus reactivity of slab two showing super and sub-critical regions of operation

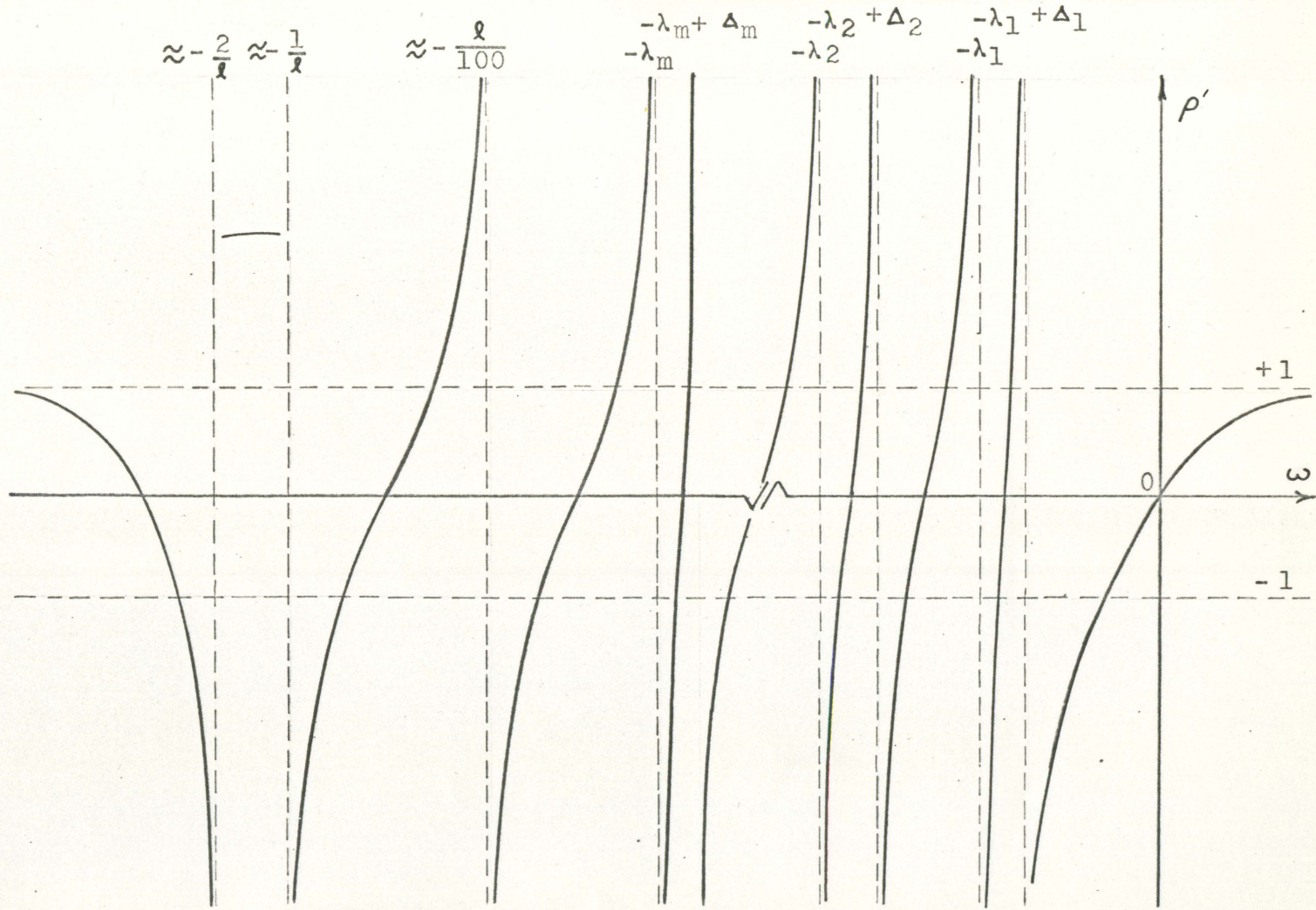


Figure 6. General ρ' versus ω plot for two slab core with m groups of delayed neutrons

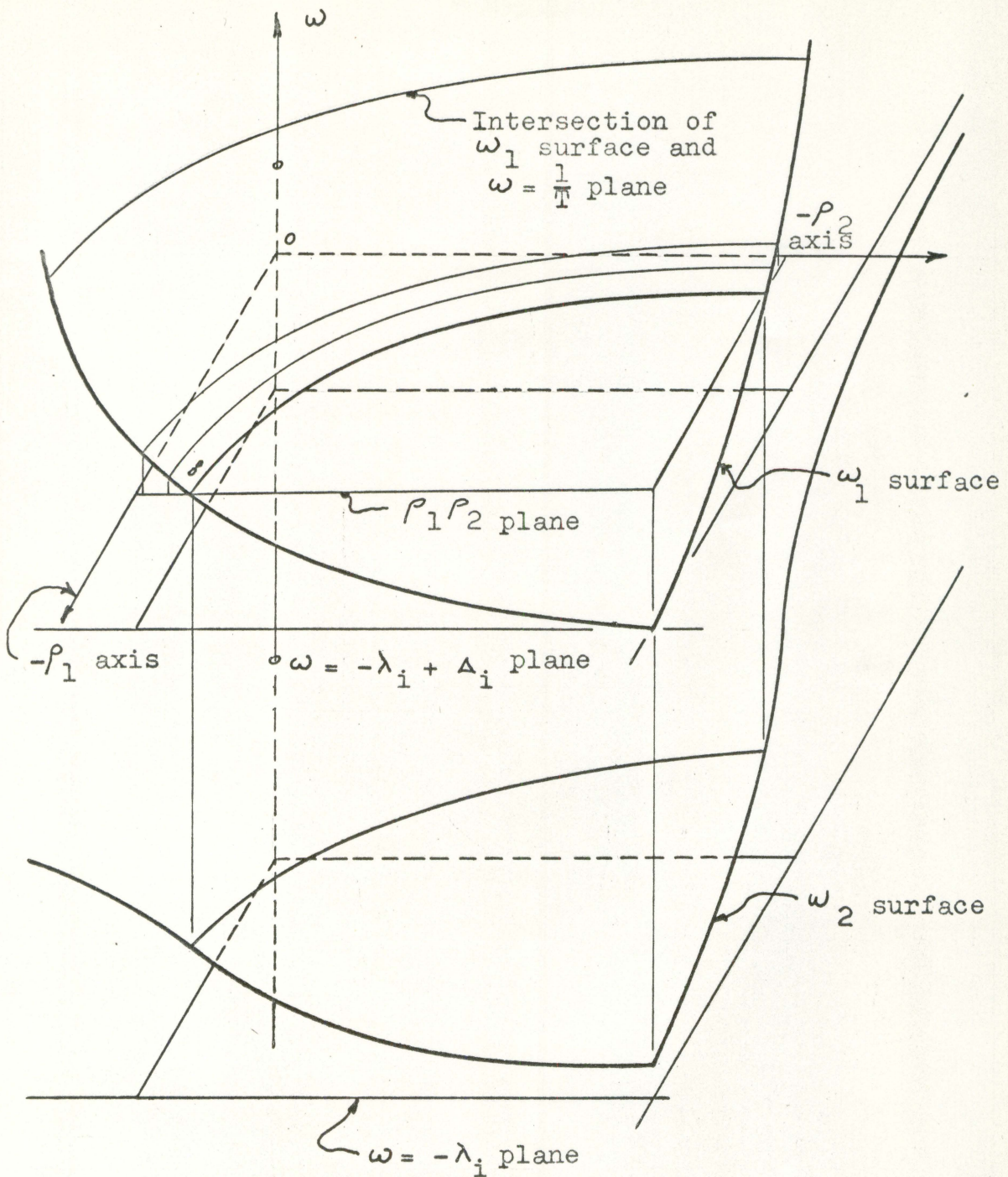


Figure 7. Three dimensional representation of $-\rho_1$ versus $-\rho_2$ versus roots, ω , of two slabs in hour equation

exist at $\omega = -\lambda_1$. In the two slab core,

$$\omega \rightarrow \pm \infty \quad \rho_1' = 1 - \rho_\infty \approx 1$$

which again closely parallels the standard inhour equation. The major difference is the presence of additional roots which originate at poles $-\lambda_1 + \Delta_1$, where Δ_1 can only be determined by rewriting Equation 13 in a factored form such that it is apparent which values of ω cause the denominator to be zero. No such form was found due to the degree and exponential nature of the equation. A three dimensional representation of Equation 13 is shown in Figure 7 for greater than $-\lambda_1$. This set of ω surfaces is analogous to the group of ω values obtained from the ordinary inhour equation and in addition accounts for reactivity changes in either or both slabs. The critical curve again is shown on the $\rho_1 \rho_2$ plane where one of the ω surfaces passes through $\omega = 0$. A general expression for the ratio of neutron densities in each slab is obtained from either Equation 12B or Equation 13B in Appendix B,

$$\frac{n_1}{n_2} = \frac{-\alpha e^{\omega \tau}}{\delta K_1 - \omega l - K_1 \sum_{i=1}^M \frac{\gamma_i \beta_i \omega}{\lambda_i + \omega}} \quad (15)$$

which reduces to

$$\frac{n_1}{n_2} = -\frac{\alpha}{\delta K_1} = -\frac{\alpha(1 - \rho_1)}{\rho_1} \quad (16)$$

for an infinite period. Thus it can be seen that the reactivity of one of the slabs sets the neutron density ratio or flux tilting between the two slabs. Movement of a control rod in one of the slabs affects the reactivity of only that slab, thus changing the flux tilting between slabs.

A positive period results when positive reactivity is added to either core when the system is originally critical. In this case, if only the positive root is considered, the curve of the resulting stable reactor period, T , is the intersection of the positive ω plane, $\omega = \frac{1}{T}$, and the three dimensional curved ω surface. The projection of a series of these intersections for several values of $\frac{1}{T}$ upon the $\rho_1 \rho_2$ plane, Figure 3A, is equivalent to the reactivity vs. period curve, Figure 2, of the one slab reactor. These curves can be applied to the UTR - 10. In using these curves for rod calibration, one first determines ρ_1 and ρ_2 for the point of critical operation, illustrated as point A. One of the rods is then withdrawn and the resulting period is measured. The worth of the rod removed is then evaluated from distance AB to be 2.69×10^{-3} . The effect of flux tilting on rod worth is seen by comparing the worth measured by establishing the same period by similar procedures from C to D where the flux tilting is 1.3 times greater and the resulting reactivity is 2.15×10^{-3} . Therefore it is necessary to know the position of both rods if

Figure 8A. Reactor period, seconds, for $\frac{\delta K_1}{K_1}$ and $\frac{\delta K_2}{K_2}$

($\alpha = 0.010$, $\beta = 0.0065$, $\gamma_{avg} = 1.034$,

$\lambda = 0.0001$ seconds, $\tau = 2.10 \times 10^{-4}$ seconds)

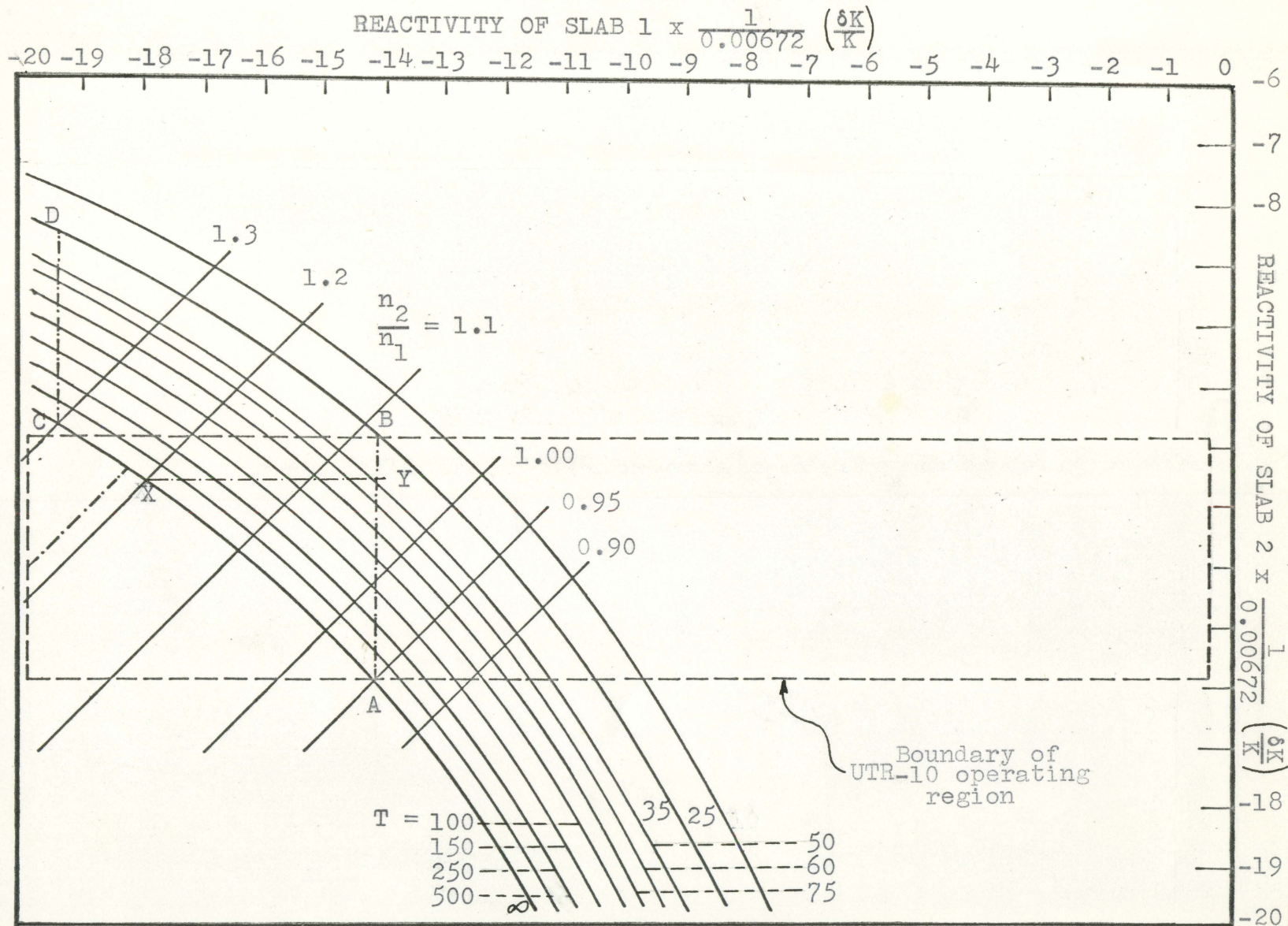


Figure 8B. Reactor periods, seconds, for $\frac{\delta K_1}{K_1}$ and $\frac{\delta K_2}{K_2}$

($\alpha = 0.009$, $\beta = 0.0065$, $\gamma_{\text{AVE}} = 1.034$,

$\lambda = 0.0001$ seconds, $\tau = 2.10 \times 10^{-4}$ seconds)

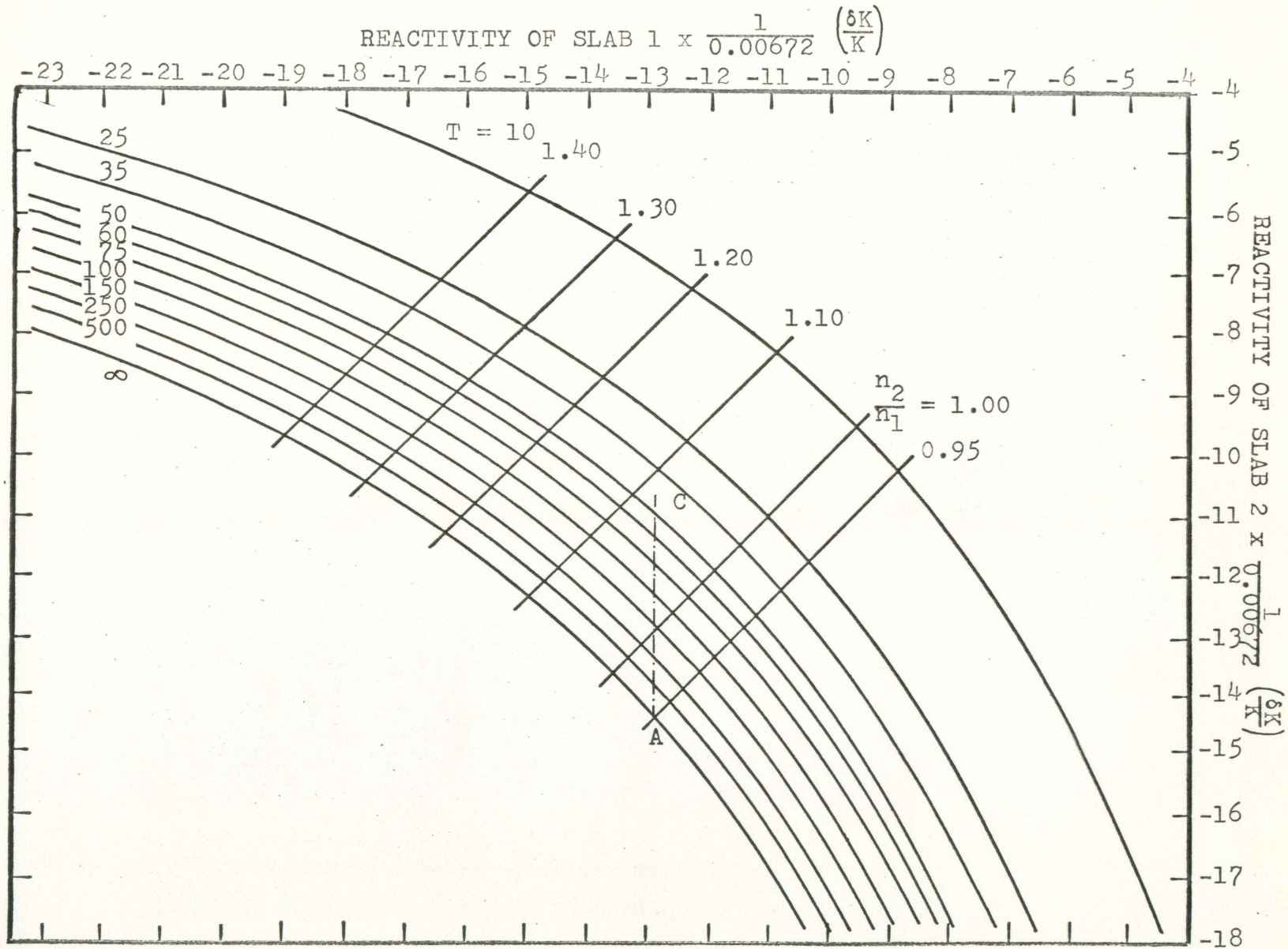
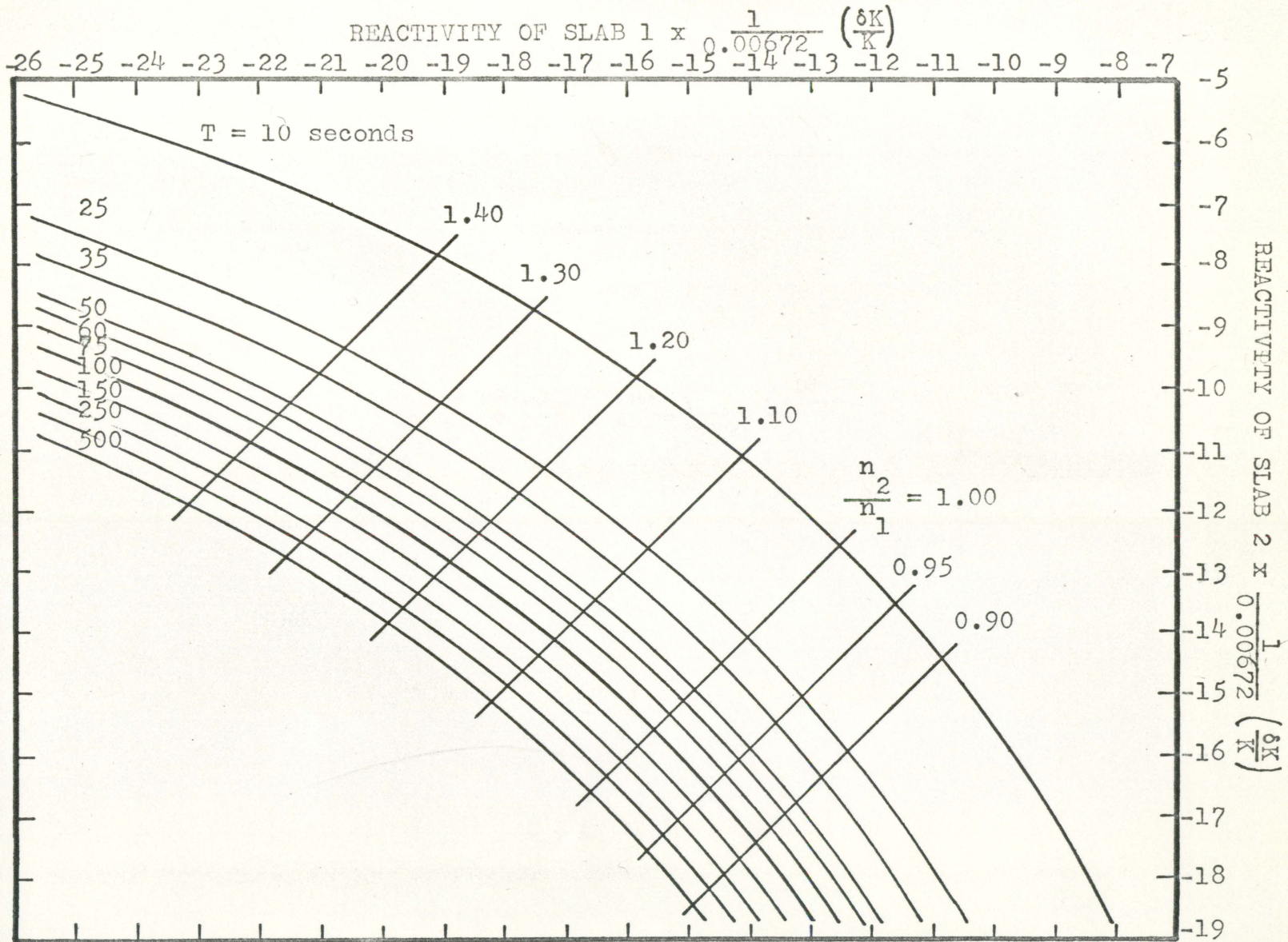


Figure 8C. Reactor periods, seconds, for $\frac{\delta K_1}{K_1}$ and $\frac{\delta K_2}{K_2}$

($\alpha = 0.011$, $\beta = 0.0065$, $\gamma_{\text{avg}} = 1.034$,
 $\lambda = 0.0001$ seconds, $\tau = 2.10 \times 10^{-4}$ seconds)



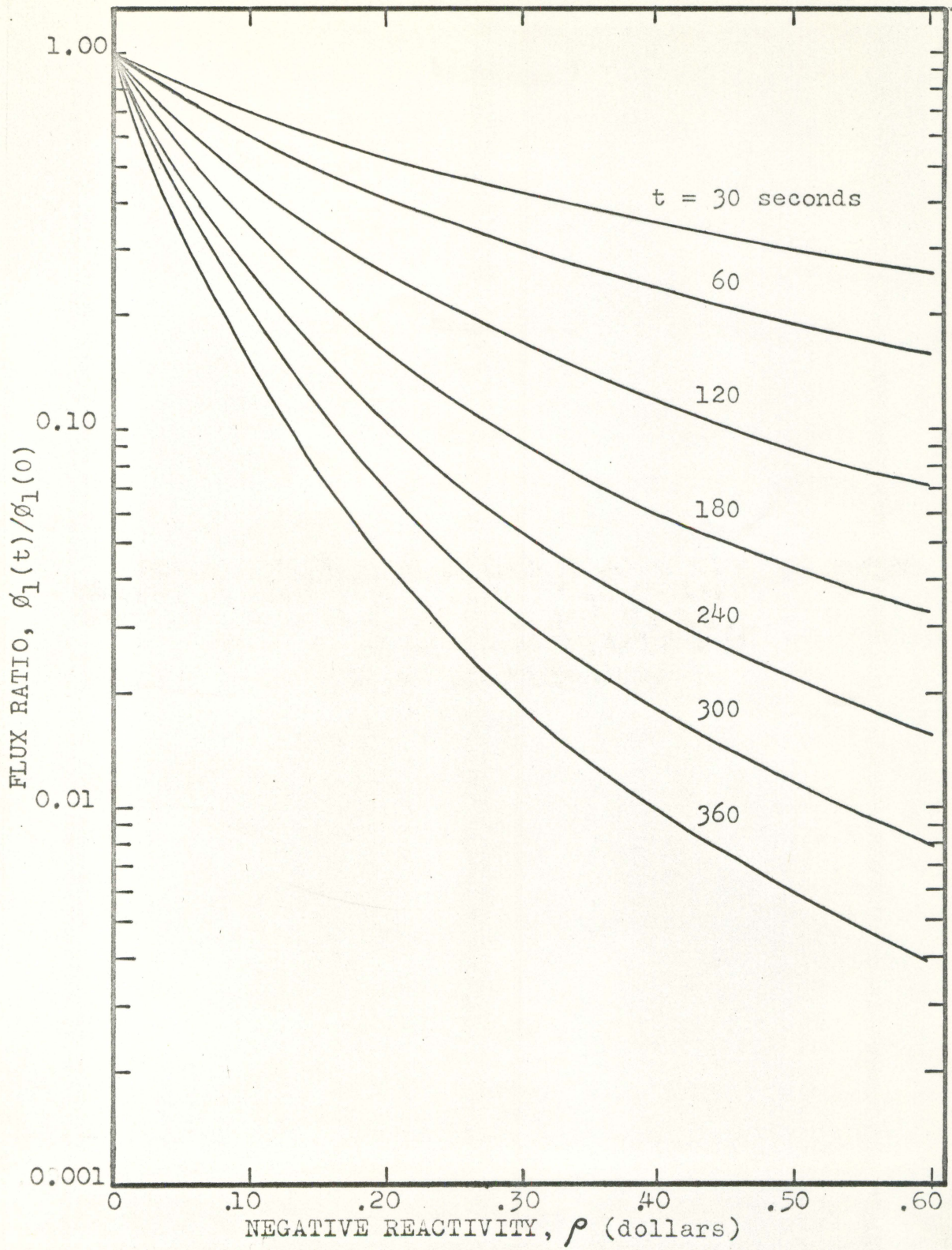
accurate rod calibration is to be achieved using positive period measurement.

For negative step inputs of reactivity into one of the slabs, all of the roots absolute value of ρ less than 1 must be considered. In this case, the $\rho = \rho_1$ plane intersects $2m + 3$ surfaces, all of which correspond to different negative values of ω . These values of ω are the roots to Equation 13 and as such can be used in a equation for the flux ratio.

$$\frac{\phi(t)}{\phi(0)} = \sum_{j=1}^{mm} A_j e^{\omega_j t} \quad (17)$$

where $mm = 2m + 3$, ω_j is one of the roots, and A_j is a constant dependent upon ρ_1 and ρ_2 and is calculated by the solution of a mm by mm matrix. Appendix C presents the assumptions and equations used to set up this matrix. Figure 9 can be used to determine negative rod worths as was explained in conjunction with Figure 3. It is important to note that Figure 9 is valid for only one value of δK_2 for the " ω "s were determined assuming that the reactivity of the opposite slab to be constant. By specifying a value of δK_2 , the neutron density ratio and corresponding critical value of δK_1 are also fixed. Significant deviations in δK_2 must be accounted for by a recalculation of " ω " and " A " terms.

Figure 9. Flux ratio in slab 1, $\phi_1(t)/\phi_1(0)$, versus negative reactivity, ρ , β at time, t , seconds after rod drop into slab 1 of a one slab core ($\alpha = 0.010$, $\beta = 0.0065$, $\gamma_{avg} = 1.034$, $l = 0.0001$ seconds, $\tau = 2.10 \times 10^{-4}$ seconds)



It should be noted that rod calibration for this type of a system could also be accomplished by taking readings of the flux tilting for consecutive critical rod positions. The procedure for such a technique would require that the reactor be made critical with the rod being calibrated completely inserted. The initial flux tilting would be measured and used with Equations 10 and 16 to determine the initial reactivity or reference reactivity of the slab containing the rod. The critical rod configuration would then be changed by withdrawing the rod being calibrated and inserting the rod in the opposite slab. Another tilt measurement would be made and a second reactivity of the slab computed. The difference between the second reactivity and the reference reactivity is the integral worth of the portion of the rod withdrawn. This process would then be repeated at successive critical rod configurations thus following the critical curve of Figure 8A. The integral worth for each position would also be evaluated. The advantage of this technique is that rod worth is determined with the reactor at a steady state condition, thus reducing considerably the number of parameters which must be considered. This method was not pursued in this thesis due to the uncertainties in the accuracy of the reactivity coupling coefficient. Also these measurements would require detectors small enough to fit between the fuel plates which are 0.40 inches apart. Gold foils would serve this purpose,

but the experimental procedures would be very time consuming since the reactor would have to be shut down and the foils removed and counted for each flux tilt measurement.

One other significant difference between the one and two slab systems is that for the coupled cores, the numerical value of the dollar is also a variable. The dollar is defined as the amount of reactivity which will cause a reactor to be prompt critical. For the prompt critical condition, the time derivative of the thermal neutron density and precursor terms in Equation 8 become zero due to the relative increase in prompt neutrons. If it is assumed that the neutron delay time between slabs, τ , is also zero, it can be shown that

$$\rho_{1\text{prompt}} = \frac{\gamma_{\text{avg}}^{\beta} - \frac{\alpha n_2}{n_1}}{1 - \frac{\alpha n_2}{n_1}} .$$

Where $\rho_{1\text{prompt}}$ is the reactivity of slab 1 required to make the system prompt critical. Using a simultaneous solution of the neutron density equations for both slabs, the relationship between K_{2p} , the prompt critical multiplication in the second slab, and $\rho_{1\text{prompt}}$ is found to be

$$\rho_{1\text{prompt}} = \frac{1}{K_{2p}(1 - \gamma_{\text{avg}}^{\beta}) + \alpha^2 - 1} \left\{ K_{2p}(1 - \gamma_{\text{avg}}^{\beta}) + \alpha^2 - 1 \right. \\ \left. - (1 - \gamma_{\text{avg}}^{\beta}) [K_{2p}(1 - \gamma_{\text{avg}}^{\beta}) - 1] \right\}$$

Note that these equations reduce to

$$\rho_{1\text{prompt}} = \gamma_{\text{avg}} \beta$$

when simplified to the one slab system with no coupling or multiplication of a second slab. This variation in the amount of reactivity constituting one dollar complicates the calibration of control rods in dollar reactivity units. It will be shown here that the amount of reactivity which must be added to achieve prompt criticality depends not only on the point of operation, as was the case in worth determinations in control rod calibrations, but also depends upon the slab in which the reactivity change is made.

The prompt critical curve is shown in Figure 10. From point A, on the critical curve, the prompt critical condition can be reached by

- a.) adding $\rho_{1\text{prompt}} - \rho_{1\infty}$ or $8.1 \times 10^{-3} \frac{\delta K}{K}$ units of reactivity, ρ_2 held constant,
- b.) adding $\rho_{2\text{prompt}} - \rho_{2\infty}$ or $15.5 \times 10^{-3} \frac{\delta K}{K}$ units of reactivity, ρ_1 held constant,
- c.) changing both ρ_1 and ρ_2 requiring the addition $7.9 \times 10^{-3} \frac{\delta K}{K}$ units of reactivity.

Note that all of these reactivity values would change if these operations were carried out at point B. This shows that the dollar reactivity unit can not effectively be applied to a two slab system unless the point of operation

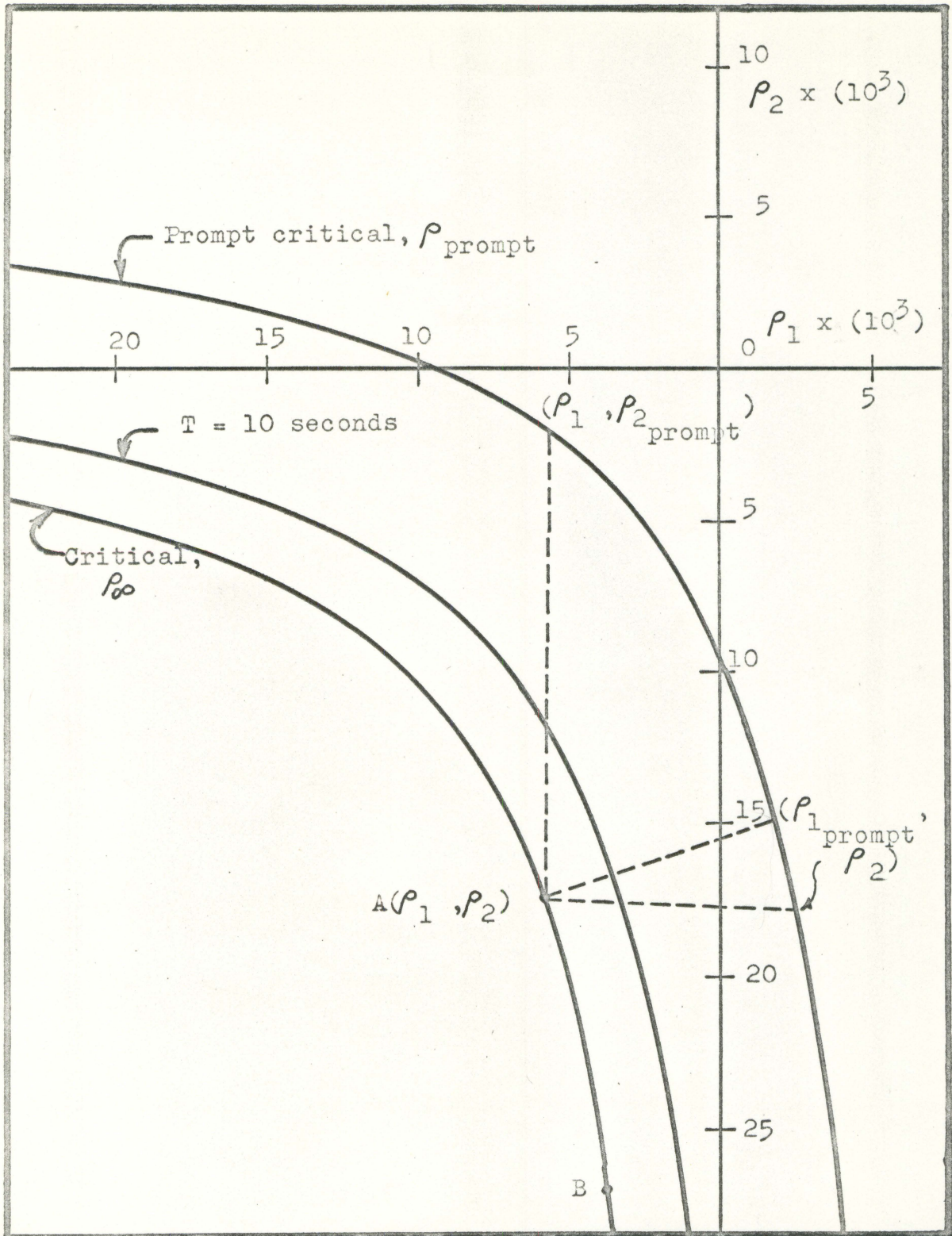


Figure 10. ρ_1 versus ρ_2 ($\alpha = 0.010$, $\beta = 0.0065$, $\gamma_{\text{avg}} = 1.034$, $\ell = 0.0001$)

and location of the reactivity change are both considered. Therefore, one dollar will be defined as the amount of reactivity which, when added to only one of the slabs, will cause the system to be prompt critical. This assumes the reactivity level of the other slab has been held constant. The dollar unit serves as a means of comparing worths between the one and two slab systems.

DESCRIPTION OF THE UTR-10 CORE AND CONTROL RODS

The UTR-10 is a heterogeneous, light water moderated, graphite reflected, 10 Kw reactor fueled with 3.0 Kg. of 90% enriched uranium-235. The central core region is shown in Figure 11. The fuel is evenly divided among 12 bundles of flat aluminum plates containing the fuel in a UAl_3 , Al matrix. There are 6 fuel bundles in each tank. Water enters the bottom of the tanks and is pumped up through the fuel regions and out of the top of the tank. The tanks are separated by 18 inches of graphite which serves as a flux trap. The Boron control rods are located against the outer side of the tanks as shown in Figure 11. Physical features of each rod are listed in Table 1. The control rods are driven by shafts extending from the control rod mount within the core to the drive motors located at the outer edge of the shield. For the shim and regulating rods, the drive shafts also turn potentiometers which provide the signal to the console position indicators.

Table 1. Physical features of UTR-10 control rods

	Dimensions inches	Distance of travel inches	Insertion time milliseconds	Drive speed inches/minute
Safety rod 1	$7 \times 7 \times \frac{1}{8}$	16	445	6.25
Safety rod 2	$7 \times 7 \times \frac{1}{8}$	16	369	6.25
Regulating rod	$2 \times 2 \times \frac{1}{8}$	16	does not drop	28.6
Shim	$7 \times 7 \times \frac{1}{8}$	16	476	6.25

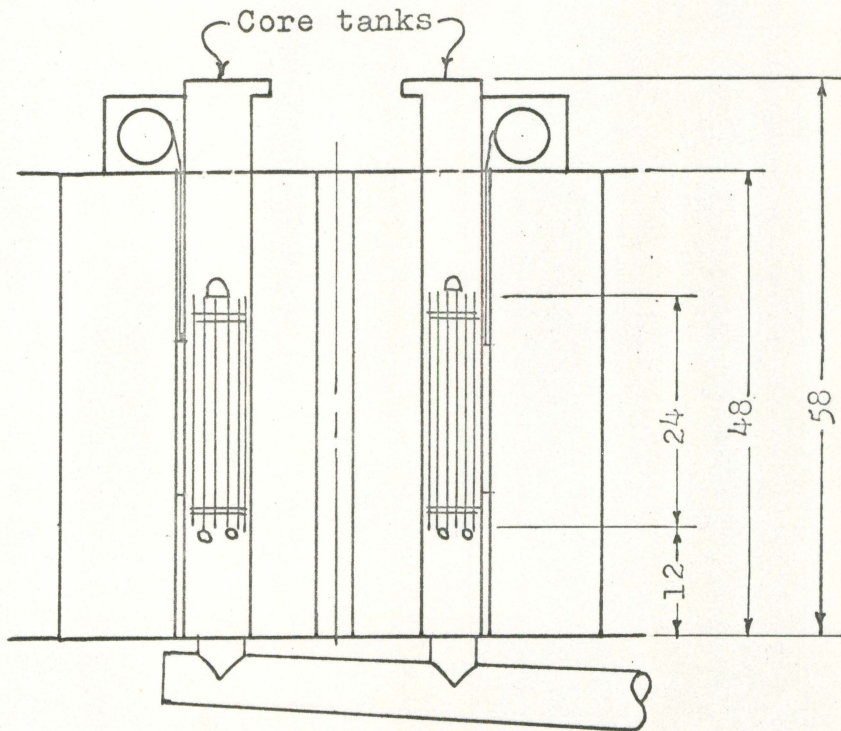
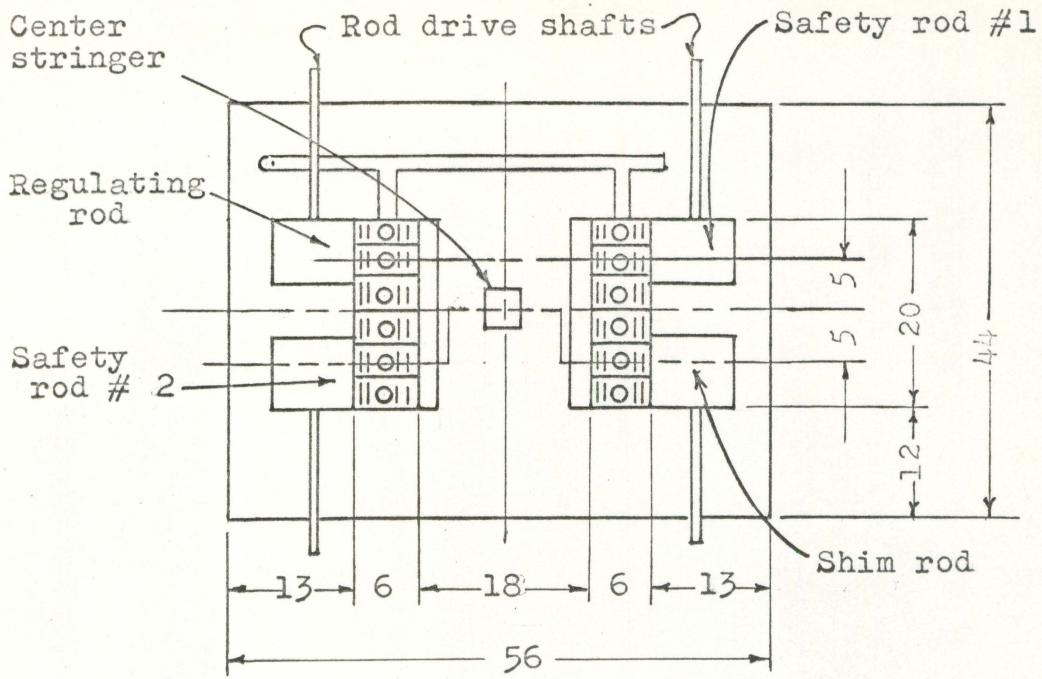


Figure 11. UTR - 10 core area

EXPERIMENTAL PROCEDURES AND RESULTS

In this section the graphs and equations of the previous sections will be applied to the calibration of control rods. Even though all measurements were made on the UTR-10's two slab core, the data was analyzed using both one and two slab core theory so that comparisons in kinetic behavior between systems could be made.

Positive Period Measurements - One Slab

As previously mentioned, the two most common techniques used in rod calibration are the rod drop and positive period measurement. In order to calibrate by positive period, the reactor is first made critical and held at one power level long enough for the delayed neutron groups to reach equilibrium concentrations. The rod is then withdrawn to a new position and the resulting stable period is measured. The incremental worth of the portion of the rod withdrawn is then determined by a computer code based upon the inhour equation with $\omega = \frac{1}{T}$. In the one slab case, Equation 6 can accurately be approximated by

$$\rho = \frac{\ell}{T} + \sum_{i=1}^m \frac{\gamma_i \beta_i}{1 + \lambda_i T} \quad (17)$$

because the prompt neutron lifetime for a thermal reactor is less than 10^{-3} seconds and T is always greater than 10 seconds.

In this work, periods were determined by measuring the doubling time from the $\gamma\gamma A$ of the UTR-10 console. The reactor power is then reduced to the initial level and the reactor is again made critical with the reg and shim-safety rods in a different position. The rod being calibrated is again partially withdrawn and the above procedure repeated. This procedure is repeated until the rod has been completely withdrawn. In order to completely withdraw the UTR-10 safety-shim rod, it was necessary to tape sheets of cadimium to the central stringer.

For this study, the incremental rod worth was determined using the Keepin and Wimmert data for delayed neutron parameters presented in Appendix D from references 10 and 11. β for this data is 0.0065 as compared to 0.0075 as determined by Hughes et al. (8). λ was taken to be 1.0×10^{-4} seconds. This parameter is free to vary over a factor of ten from this value when small values of reactivities are being considered, without significant differences in rod worths resulting.

The experimental accuracy of measuring reactivity based on asymptotic period measurement is discussed by Toppel (12). For a reactor with a prompt neutron lifetime of 10^{-4} seconds, one obtains asymptotic measurements which are 99% accurate 70 seconds after the reactivity change is made. This one per cent error introduces only a difference of $\pm 7.8 \times 10^{-2}$ cents worth or $5.87 \times 10^{-4} \% \Delta K/K$ in a differential worth of 9.95 cents. This is an error of only 0.783 %, which is

insignificant.

The differential rod worth curve is next constructed and integrated to give the integral shim-safety rod worth curve shown in Figure 12A. Experimental data and calculated results are given in Table 2. Figure 12B is the integral curve for the reg rod.

Rod Drop Method - One Slab

The rod drop calibration technique follows this basic procedure:

1. The reactor is brought to a power level where gamma compensation current will not affect power level readings.
2. The reactor is made critical with the rod which is being calibrated fully or partially withdrawn.
3. The rod is dropped into the core, making the reactor subcritical thus causing the flux level to decrease.
4. The decay of the flux level is recorded. Data taken from the UTR-10 Am meter is given in Table 3.
5. The reactor is again made critical with the control rods at a different position and the above procedure repeated for increments over the entire rod.
6. The integral worth of the portion of the rod dropped into the core is obtained from an evaluation of Equation 4 as graphically presented in Figure 3.

The total integral worth curve as measured by this method is also shown in Figure 12A, and is appreciably higher than measurements made by positive periods. This

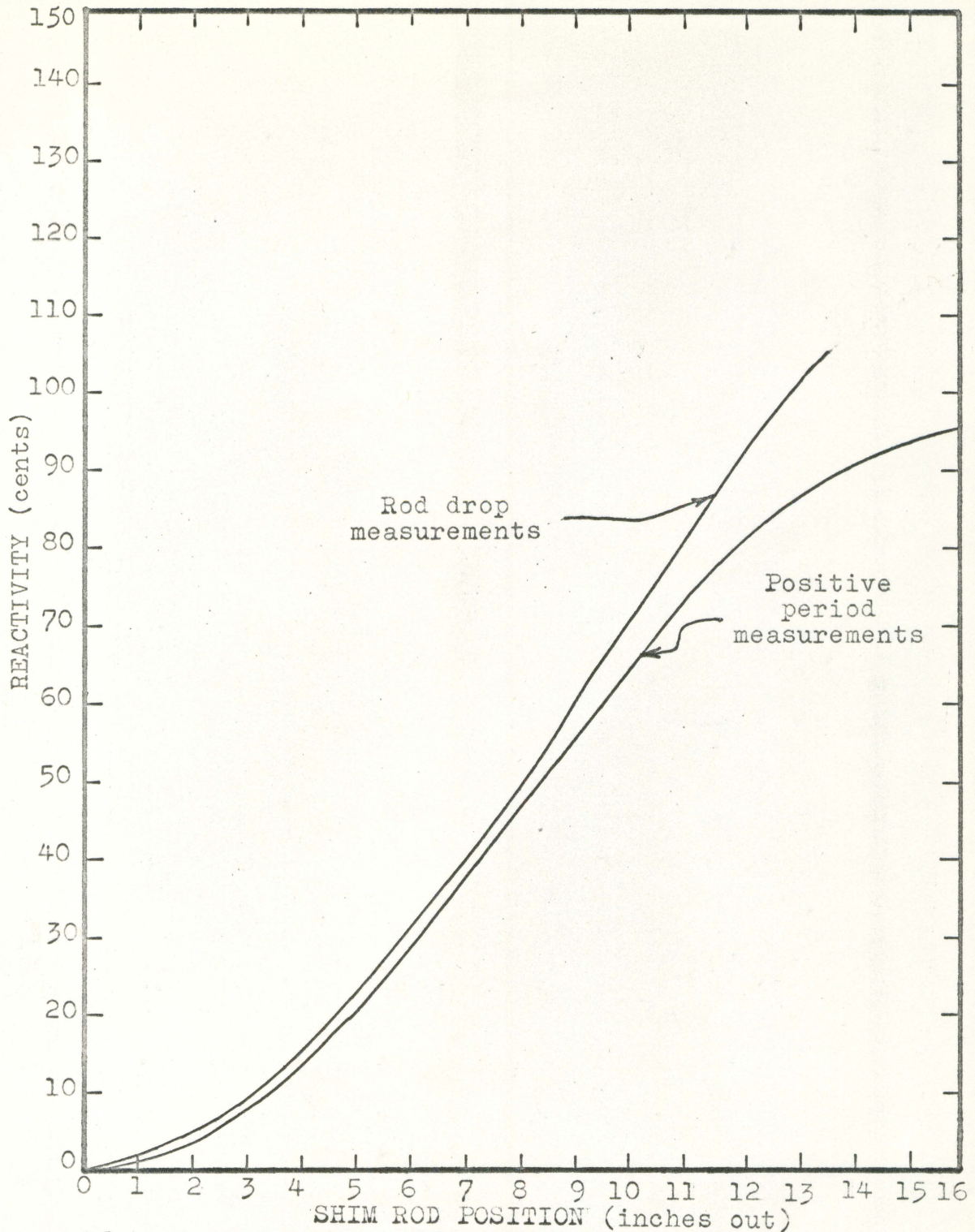


Figure 12A. One slab integral reactivity worth of UTR - 10 shim rod based on positive period and rod drop measurements ($\rho = 0.0065$, $\gamma_{avg} = 1.034$, $\lambda = 0.0001$ seconds)

Table 2. One slab reactivity worths of shim rod based on positive period measurements^a

Shim rod position inches		Stable period seconds	Worth cents	Integral worth at midpoint of interval cents
Initial	Final			
2.60	4.50	92.8	10.32	9.66
4.05	6.00	56.4	14.85	19.28
5.50	7.25	45.2	17.25	32.91
7.00	8.50	68.5	12.96	45.64
7.85	9.50	62.3	13.88	53.56
9.00	10.50	68.2	13.00	62.70
10.00	12.00	43.4	13.83	72.44
11.20	13.00	66.1	13.30	80.31
11.80	14.50	62.3	13.88	86.89
13.48	16.00	149.8	7.05	93.20

^a $\beta = 0.0065$, $\gamma_{avg} = 1.034$, $\lambda = 0.0001$ seconds.

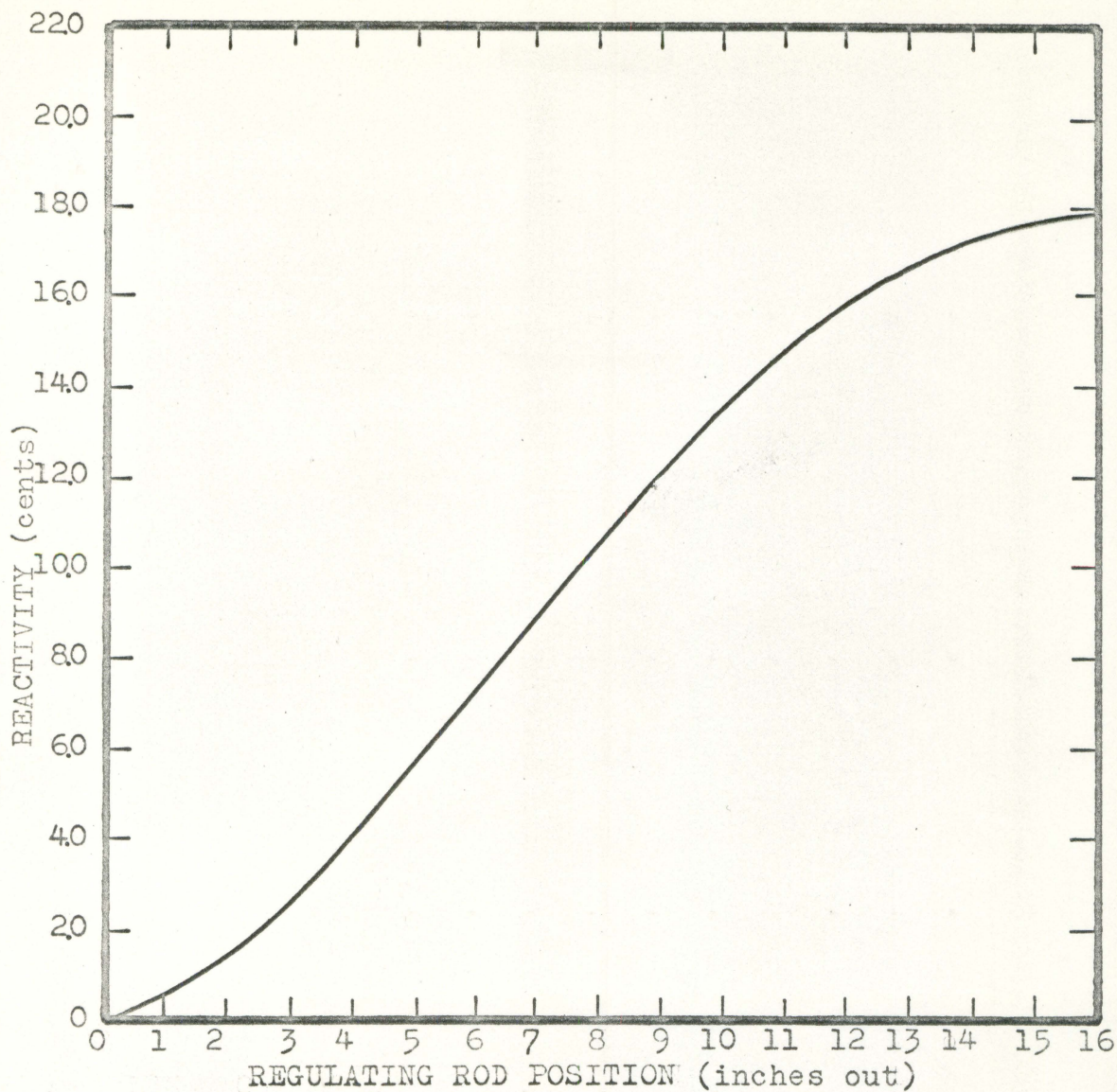


Figure 12B. One slab integral reactivity worth of UTR - 10 regulating rod based on positive period measurements ($\beta = 0.0065$, $\gamma_{\text{avg}} = 1.034$, $\lambda = 0.0001$ seconds)

Table 3. Typical data of rod drop experiments from initial power level of 150 watts assuming a one slab reactor^a

Initial shim rod position inches out	Power level watts at time t seconds after rod drop				Integral worth cents
	time after rod drop seconds				
	30	60	180	240	
2.80	107.0	90.7	47.2		8.0
4.00	83.1	61.3	21.4	13.0	16.0
7.05	43.8	26.2	4.75		40.0
9.05	30.0	16.3	2.41		62.5
11.10	23.1	12.0	1.60	0.587	81.0
13.50	7.45	3.75	0.395	0.172	106.5

^a $\beta = 0.0065$, $\gamma_{avg} = 1.034$, $\lambda = 0.0001$ seconds.

Table 4. One slab reactivity worths of the regulating rod based on positive period measurements^a

Regulating rod position inches		Stable period seconds	Worth cents	Integral Worth at midpoint of interval cents
Initial	Final			
0.0	2.0	749	1.65	0.39
1.0	3.0	525	2.30	1.37
2.0	4.0	461	2.60	2.57
3.0	5.0	430	2.78	
3.0	5.0	335	3.49	3.93
3.0	5.0	367	3.21	
4.0	6.0	426	2.80	5.43
5.0	7.0	329	3.55	7.07
5.0	7.0	346	3.39	
6.0	8.0	332	3.52	
6.0	8.0	343	3.42	8.79
7.0	9.0	365	3.23	10.48
8.0	10.0	384	3.08	12.08
9.0	11.0	354	3.32	13.59
9.0	11.0	404	2.94	
10.0	12.0	485	2.48	14.94
11.0	13.0	557	2.18	16.09
12.0	14.0	1072	1.17	16.88
10.0	16.0	630	1.94	17.37
0.0	16.0	38.7	19.11	19.11

^a $\beta = 0.0065$, $\nu_{avg} = 1.034$, $l = 0.0001$ seconds.

discrepancy will be explained later in the light of two slab core theory.

Positive Period Measurement - Two Slabs

The general procedures of determining rod worth in a two slab core are basically the same as outlined for the one slab case. However, before making a calibration, the coupling coefficient for the system and the point of operation on a corresponding $\rho_1 - \rho_2$ diagram similar to Figure 8A must be determined. To determine the point of operation, it is required that either ρ_1 and ρ_2 or the flux tilting and its corresponding period be known. The latter approach was utilized through foil measurements to determine the maximum and minimum values of the flux tilting at criticality. The upper limit, BC of Figure 8A, is set by complete withdrawal of the regulating rod and the lower limit, A, occurs at total insertion. Bare gold foils were irradiated in both core tanks simultaneously for the extreme regulating rod positions. A third set of cadmium covered foils was irradiated with the regulating rod inserted and the results used to correct the other two sets of foils for epi-thermal neutron activation. The data from this experiment is given in Tables 5A and 5B. The results of these measurements serve to indicate that the ratio of thermal neutron flux in the slab containing the regulating rod to that in the slab containing the shim rod varies from 0.95, when the regulating rod is completely

Table 5A. Thermal neutron activation of gold foils -
regulating rod completely inserted^a

Position fuel element number	Specific activity ^b counts/minute - gram	Cadmium ratio
N-3	253,938	3.178
N-4	254,847	3.226
N-5	310,885	3.902
Average	273,223	
S-3	283,575	3.345
S-4	214,909	2.764
S-5	283,801	3.690
Average	260,229	

^aShim rod at 5.3 inches out, power level 10 watts for
5 minutes.

^bCorrected for cadmium ratio.

$$\frac{n_2}{n_1} = \frac{\text{Average thermal activity in south slab}}{\text{Average thermal activity in north slab}} = \frac{260,229}{273,223} = 0.954$$

Table 5B. Thermal neutron activation of gold foils -
regulating rod completely withdrawn^a

Position fuel element number	Specific activity ^b counts/minute - gram
N-3	250,545
N-4	236,149
N-5	231,672
Average	239,455
S-3	299,612
S-4	306,732
S-5	303,522
Average	303,280

^aShim rod at 2.6 inches out, power level 10 watts for
5 minutes.

^bCorrected for same cadmium ratios as Table 5A.

$$\frac{n_2}{n_1} = \frac{\text{Average thermal activity in south slab}}{\text{Average thermal activity in north slab}} = \frac{303,280}{239,455} = 1.27$$

inserted, to 1.27, with the regulating rod withdrawn. All other points of operation lie between these values and can be approximated by consideration of the regulating rod position and the expected regulating rod integral worth curve. The boundaries of the UTR-10 operating region are shown in Figure 8A. The right and left boundaries were obtained after determining the worth of the shim rod.

As mentioned above, an appropriate value of the reactivity coupling coefficient, α , must also be determined. This parameter has considerable effect on the location of the critical curve on $\rho_1\rho_2$ plane. Decreasing the coupling shifts the critical curve closer to the origin and also increases the periods obtained as a result of positive changes in reactivity. For example, consider Figure 8B, based upon alpha equal to 0.0009. If the reactor were critical at point A with the regulating rod completely inserted, and then made supercritical by complete withdrawal of the regulating rod to point C, the expected period would be 43 seconds. In the UTR-10, this procedure causes a period between 34.0 and 38.7 seconds depending upon moderator temperature. Alpha must be determined such that this measured period corresponds to the period predicted by point C. For a period of 35.0 seconds, this condition is satisfied with alpha equal to 0.010. Previous determinations of alpha range from 0.008, Danofsky (4), to 0.0155.¹ The validity of this procedure was checked by other period measurements,

¹Crews, Ray F., Mountain View, California. Reactivity data. Private communication to Dr. Glenn Murphy. 1959.

which were found to agree with predicted periods within 5%.

From these measurements, the total worth of the regulating rod was determined to be \$0.217 as compared to \$0.180 by the one slab core approach. Note also from Tables 4 and 6 that when the regulating rod is completely withdrawn, the resulting period predicts a two slab worth of 22.49 cents which differs from the incremental total by 0.8 cents. One slab theory predicts a worth of 19.11 cents or a difference of 1.11 cents. This discrepancy is explained in the conclusions. The integral worth curve of the regulating rod is shown in Figure 13A. Complete withdrawal of the shim rod was not possible due to the short period which would have resulted. Figure 13B shows the shim rod integral worth curve for the portion which could be withdrawn without adding poison to the core. Extrapolation of this curve based upon the positive period measurements and boundaries of operation of Figure 8A for the regulating rod at 8.0 inches predicts the worth of the rod to be \$1.26 as compared to \$0.96 for the one slab measurements.

The introduction of poison to the core to make complete withdrawal possible must be done in such a way so as not to vary alpha. It appears that this variation could be avoided by distributing poisons in the fuel bundles. Placing cadmium on the central stringer as was done in assuming a one slab loading essentially shadows one slab from the other and thus decreases the interaction between them which is a decrease

Table 6. Two slab reactivity worths of the regulating rod based on positive period measurements^a

Regulating rod position inches		Shim rod position inches	Stable period seconds	Worth cents	Integral Worth at midpoint of interval cents
Initial	Final				
0.0	2.0	5.85	749	2.06	0.64
1.0	3.0	5.80	525	2.86	1.86
2.0	4.0	5.50	461	3.20	3.37
3.0	5.0	5.10	430	3.39	
3.0	5.0	5.50	335	4.25	5.06
3.0	5.0	5.50	367	3.92	
4.0	6.0	5.10	426	3.40	6.87
5.0	7.0	5.00	329	4.27	
5.0	7.0	4.60	346	4.08	8.85
6.0	8.0	4.50	332	4.21	
6.0	8.0	4.90	343	4.09	10.90
7.0	9.0	4.20	365	3.84	12.96
8.0	10.0	4.00	384	3.65	14.82
9.0	11.0	3.90	354	3.90	16.60
9.0	11.0	4.06	404	3.46	
10.0	12.0	3.40	485	2.91	18.14
11.0	13.0	3.10	557	2.54	19.26
12.0	14.0	3.20	1072	1.36	20.26
12.0	16.0	3.20	630	2.25	20.96
0.0	16.0	5.80	38.7	22.49	22.49

^a $\alpha = 0.010$, $\beta = 0.0065$, $\gamma_{avg} = 1.034$, $l = 0.0001$ seconds, $\tau = 2.10 \times 10^{-4}$ seconds.

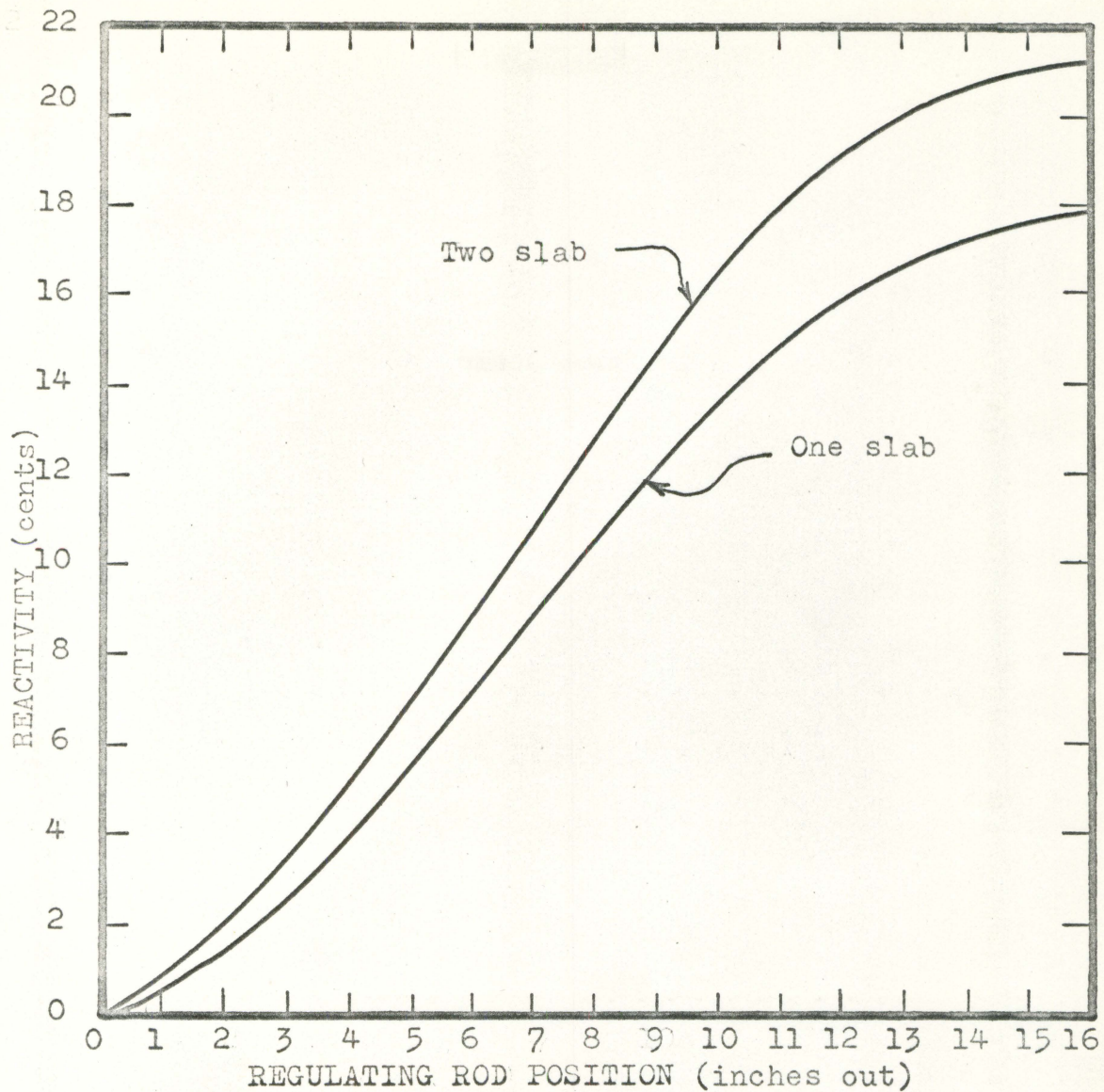


Figure 13A. One and two slab integral reactivity worth of the UTR - 10 regulating rod based on positive period measurements ($\alpha = 0.010$, $\beta = 0.0065$, $\gamma_{\text{avg}} = 1.034$, $\lambda = 0.0001$ seconds)

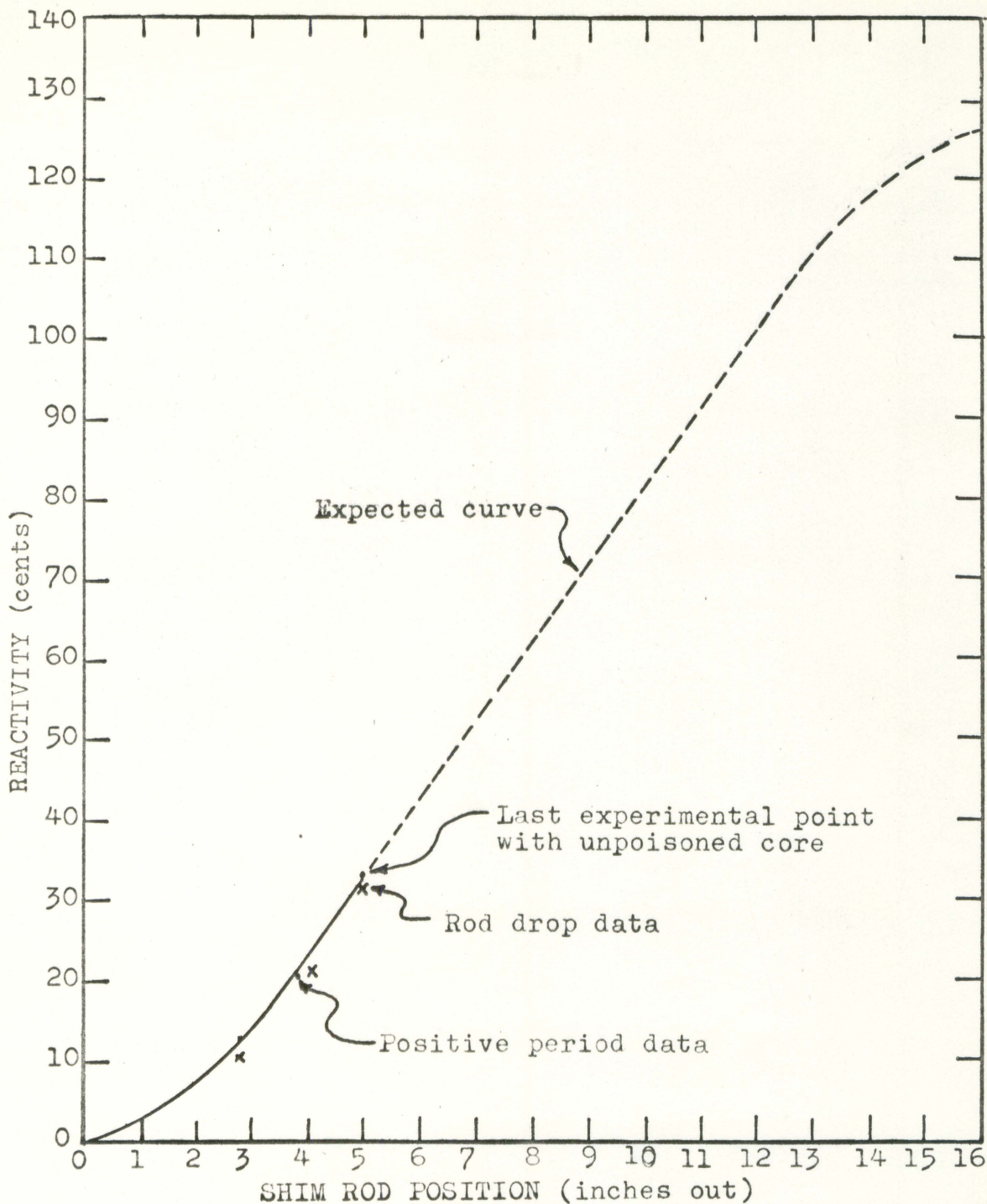


Figure 13B. Two slab integral reactivity worth of UTR - 10 shim rod based on positive period and rod drop measurements ($\alpha = 0.010$, $\beta = 0.0065$, $\gamma_{\text{avg}} = 1.034$, $l = 0.0001$ seconds, $\tau = 2.1 \times 10^{-4}$ seconds)

in alpha.

Rod Drop Method - Two Slabs

The rod drop calibration technique in the two slab core is the same as in the one slab core once the coupling coefficient and point of operation have been determined as explained in the previous paragraphs. The calibration data obtained from the portion of the sim rod which could be withdrawn without poisoning the core is given in Table 7 and the integral worth curve plotted in Figure 13B. The regulation rod can not be calibrated by this technique because it can not be dropped.

Table 7. Two slab reactivity worths of the shim rod based on positive period measurements^a

Regulating rod position inches	Shim rod position inches		Stable period seconds	Worth cents	Integral worth at midpoint of interval cents
	Initial	Final			
16.0	2.25	3.50	173.9		
16.0	2.15	5.40	37.52	10.3	12.9
8.0	3.50	6.50	30.3	31.9	20.9
				32.0	33.0

^a $\alpha = 0.010$, $\beta = 0.0065$, $\nu_{avg} = 1.034$, $\lambda = 0.0001$ seconds, $\tau = 2.10 \times 10^{-4}$ seconds.

Table 8. Two slab reactivity worths of the shim rod based on rod drop measurements^a

52

Shim rod position before drop inches out	Regulating rod position before drop ^b inches out	Integral worth of portion dropped cents
2.80	8.0	-10
4.15	8.0	-21
5.00	7.3	-31

^a $\alpha = 0.010$, $\beta = 0.0065$, $\nu_{avg} = 1.034$, $\tau = 2.10 \times 10^{-4}$ seconds, $\lambda = 0.0001$ seconds.

^b = Regulating rod assumed to be at 8.0 inches = out for computer solution.

COMPARISONS AND CONCLUSIONS

Although control rod calibration has been the primary concern in this study, it is of interest to compare the general behavior as well as the calibration results for the one and two slab core systems.

One of the differences between the two systems is the relative magnitudes of measured reactivities. It has been found experimentally that low values of positive and negative worth measurements generally agree when compared within the same system. However, there is no such comparison between systems. For example, in the one slab system, theoretically an addition of $\$0.16$ would result in a period of 50 seconds. In the two slab system, this amount would only produce periods between 60 and 180 seconds depending upon the flux tilting, coupling coefficient, and value of the dollar. Therefore such an approach to a worth comparison is not correct. The only link between the systems is the similarity in behavior under equal initial conditions. Figure 14 shows the decay of the flux ratio as a function of time after the same area of control rod has been dropped into both systems. Initially the flux in the two slab system is tilted such that the n_1/n_2 ratio is only 1.09. Note that even though the worths inserted are different, the resulting behavior is generally the same and both successfully predict the actual behavior for the same duration after the drop. Similarly,

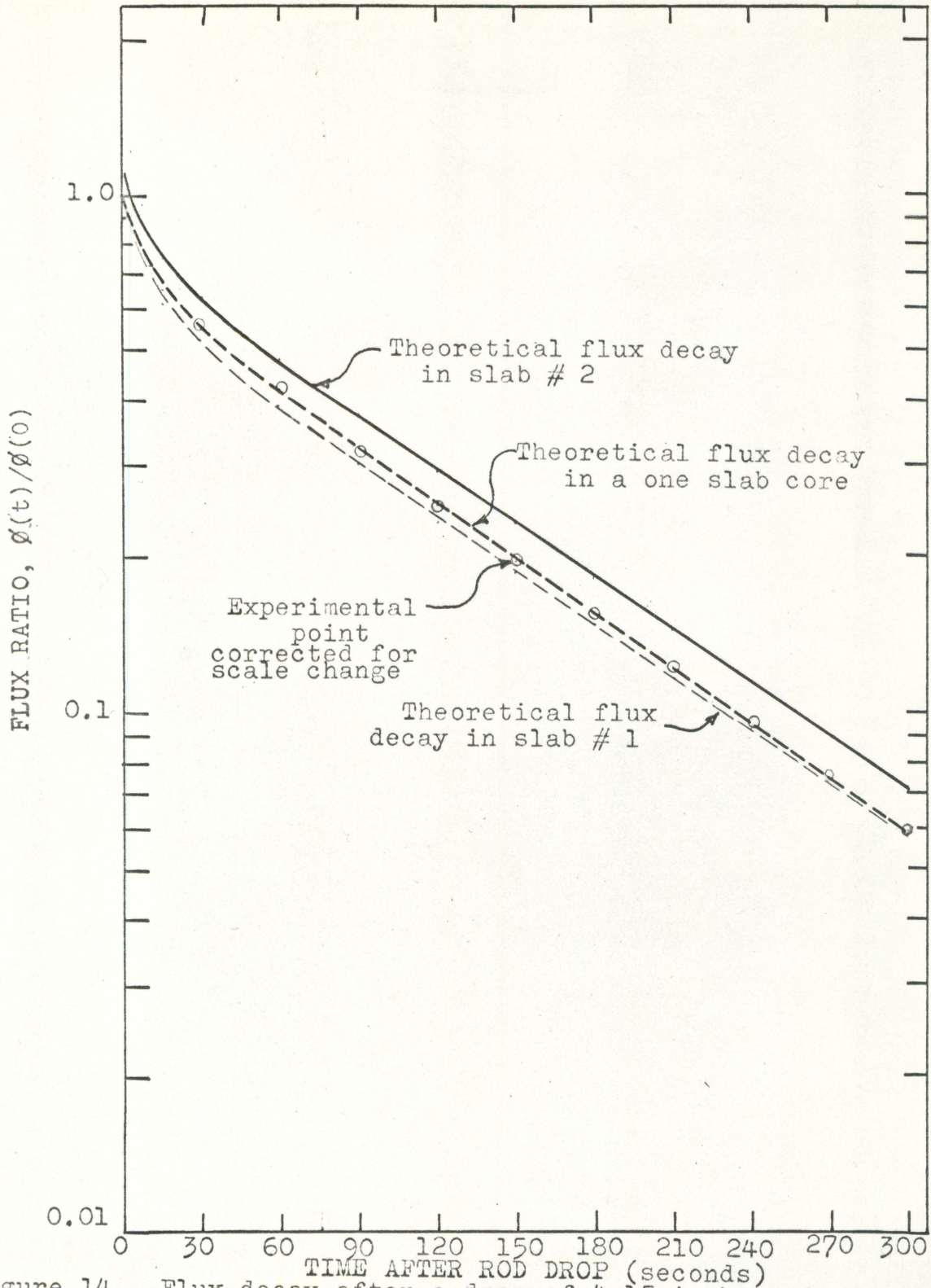


Figure 14. Flux decay after a drop of 4.15 inches of shim rod into slab one

for positive period measurements, two slab worths, 1.5 times greater than those of the one slab model, produce equal periods. Thus, this magnitude difference between systems is justified.

It was noted earlier that negative insertion measurements gave higher values of rod worth than measurements made by positive periods. This discrepancy in worths, based on the one slab model, can not solely be attributed to variations in the reactivity coupling coefficient due to the addition of poisons. The effect of alpha variations on the predicted transient behavior has already been noted and deviations from a smooth integral worth curve are to be expected. However, it seems that for a given model and a given value of coupling, equal values of positive and negative reactivity insertions should be measured as equals. Neither approach should be more sensitive to changes in alpha for both methods are based on the same equations. Two basic differences in the experimental procedure account for this discrepancy, both of which are results of flux tilting which is not considered by the one slab reactor model. 1) Positive period measurements are made over small increments of reactivity. For the shim rod, these measurements are always made in such a direction that n_2/n_1 decreases. This procedure is shown in Figure 8A by path XY in which the flux ratio decreased from 1.20 to 1.05. 2) Rod drop measurements of the shim may vary over larger increments of worth than the positive period increments and are always made such that n_2/n_1 increases. Thus when a rod

is dropped into slab 1, the flux ratio increases as the power level decreases and approaches the tilting value at the new point of operation as shown in Figure 8. Figure 15 shows the increase in tilting as a function of time for the rod drop into the two slab system shown in Figure 14, where initially the flux ratio was 1.091. Figure 8A predicts the tilting to be approximately 1.22 which agrees with that obtained. The point to be noted is that when a large portion of a rod is dropped into a two slab core, as the overall flux level decreases, the flux level in the slab receiving the rod decreases more rapidly than that in the other slab. One slab theory can not account for tilting, therefore, this increase in the rate of flux level decay would indicate that an apparently larger amount of reactivity had been added than was actually the case. It is seen in Figure 14 that the flux ratio decay of the one slab model more closely follows the decay of slab 1 which received the rod. Thus, in applying experimental results from a two slab reactor to the one slab model, the worth which is derived from flux decay with no tilting would actually be based on the behavior of slab 1. But because of the increase in the tilting the flux ratio decreases more rapidly. Therefore one slab theory assigns a greater worth to the rod than it would have had the rod been dropped into a one slab reactor. And furthermore, as the amount of reactivity dropped into slab 1 increases, the equilibrium value of n_2/n_1 becomes larger

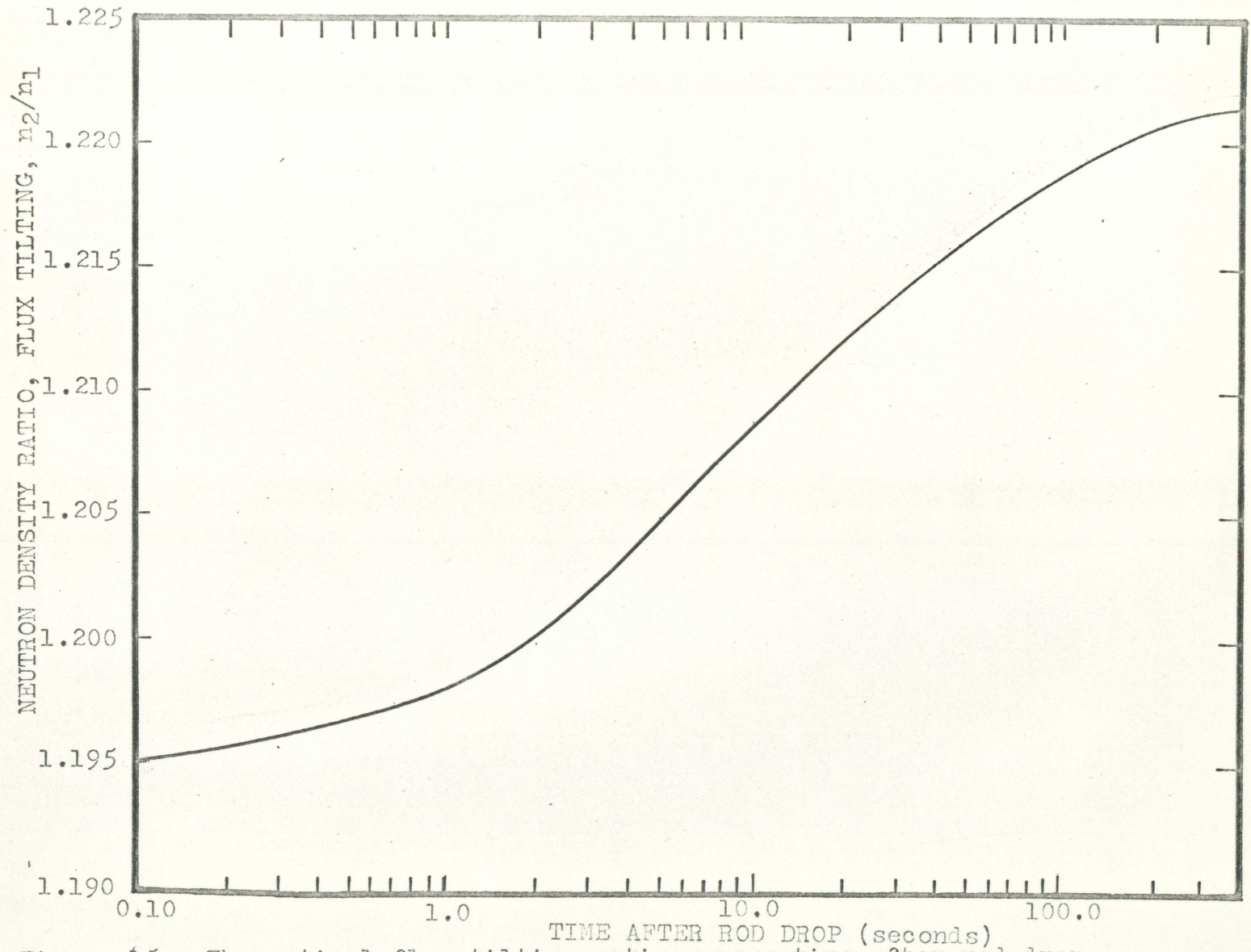


Figure 15. Theoretical flux tilting ratio versus time after rod drop

thus magnifying its true worth in a one slab system.

A similar magnification in measured worths is observed for positive reactivity insertions. It was noted earlier that the integral worth of the regulating rod as determined by incremental withdrawals was one cent less than that measured by withdrawing the entire rod at once. This difference can again be attributed to time change of the tilting ratio. When the small portion of the rod were withdrawn, the neutron density ratio was increased only slightly. However, in the case of complete removal, the ratio was to change from 0.95 to a steady state value of 1.27. This requires the neutron density in the slab containing the regulating rod to increase faster than the density in the opposite slab. This additional increase in neutron density would be detected as a shorter period than would result had constant tilting been assumed. This shorter period would be attributed to a greater rod worth in either system. Two slab theory as applied to the analysis of positive periods was based only on one positive root and therefore was not able to compensate for all of this change.

In general, it can be concluded that when large control rod worths are being measured in a two slab system, consideration must be given not only to reactivity coupling variations and flux tilting, but also to the growth or decay of the neutron density ratio.

SUGGESTIONS FOR FURTHER STUDY

1. Consider the effect of higher harmonic neutron waves on reactivity worths and the neutron density ratio transient.
2. Make measurements of reactivity worths by measuring the flux tilting at various rod positions.
3. Consider spatial effects of rod position and detector location on reactivity measurements.
4. Develop kinetic equations which describe the multi-region system which are less dependent upon exact measurement of the coupling coefficient.

LITERATURE CITED

1. Avery, R. Theory of coupled reactors. International Conference on the Peaceful Uses of Atomic Energy, 2nd, Geneva, 1958 Proc. 15: 1858-1868. 1958.
2. Baldwin, G. C. Kinetics of a reactor composed of two loosely coupled cores. Nuclear Science and Engineering 6: 320-327. 1959.
3. Baldwin, G. C., Carey, Walter E., Gilesiz, Ayhan, Kimel, William R., Klaiber, G. Stanley, Pawlicki, Gerald S., and Prohammer, Fredric G. Pedogogical applications of an Argonaut reactor. U.S. Atomic Energy Commission Report ANL 5989 [Argonne National Laboratory, Lemont, Illinois]. [ca.] 1961..
4. Danofsky, Richard A. Kinetic behavior of coupled reactor cores. Unpublished M.S. thesis. Ames, Iowa, Library, Iowa State University of Science and Technology. 1961.
5. Glasstone, Sammuell and Edlund, Milton C. The elements of nuclear reactor theory. New York, N.Y., D. Van Nostrand Co., Inc. 1952.
6. Harrer, Joseph M. Nuclear reactor control engineering. New York, N.Y., D. Van Nostrand Co., Inc. 1963.
7. Henry, A. F. and Curlee, N. J. Verification of a method for treating neutron space time problems. Nuclear Science and Engineering 4: 727-744. 1958.
8. Hughes, D. J., Dabbs, J., Cahn, A., and Hall, D. Delayed neutrons from fission of uranium 235. Physics Review 73: 111-128. 1948.
9. Keepin, G. R. Physics of nuclear kinetics. Reading, Mass., Addison-Wesley Publishing Co., Inc. 1965.
10. Keepin, G. R. Reactor kinetics and control. U.S. Atomic Energy Commission Report TID 7662. Division of Technical Information Extension, AEC 1964.
11. Keepin, G. R., Wimett, T. F., and Zeigler, R. K. Delayed neutrons from fissionable isotopes of uranium, plutonium, and thorium. U.S. Atomic Energy Commission Report LA 2118 [Los Alamos Scientific Laboratory, Los Alamos, New Mexico] . 1958.

12. Toppel, B. J. Errors in reactivity calculations by means of asymptotic period measurements. Nuclear Science and Engineering 5: 88-99. 1959.

ACKNOWLEDGMENTS

The author wishes to express his sincere appreciation to Dr. Richard A. Danofsky for his help, suggestions, and stimulating interest in this project.

APPENDIX A

Computer Solutions and Flow Sheets

This section presents the computer solutions used in this study for negative insertions reactivity into the one and two slab systems.

Negative Insertions into a One Slab Reactor

Main program

The flow diagram describing the main program is given in Figure 16. The input arrays and parameters are defined as follows:

- T - an array of times after insertion of negative reactivity
- B - Delayed neutron group abundance ratios
- DC - Decay constants of delayed neutron groups
- G - Fission effectiveness of delayed neutron groups
- APNL - an array of prompt neutron lifetimes
- BCD - Alphameric information used in plotting routines.
- II - Number of delayed neutron groups to be considered
- JJ - Number of prompt neutron lifetimes to be considered
- TB - Total delayed neutron fraction
- JK - Number of times to be considered
- RHOMA - Maximum absolute value of negative reactivity
- RHOMI - Minimum absolute value of negative reactivity
- DELTA - Increment of reactivity

GAVG - Average of the fission effectiveness of all delayed neutron groups

This diagram does not show the generation of the RHO and effective array H(I) or plotting program. Basically this program performs the following functions:

- (1) Collects input data and stores it for later use.
- (2) Determines number of values of reactivity for which it will compute output parameters.
- (3) Computes useful arrays, RHO and effectiveness array.
- (4) Calls subroutines FIRST, HUNT, and RHOS to determine roots of inhour equation.
- (5) Calls ANSER to determine coefficients for flux ratio summation.
- (6) Calculates the flux ratio, ϕ/ϕ_0 , for the times imputed, T array, over the range of negative reactivities of interest.
- (7) Writes output in labeled and orderly form.

The program was written in a versatile form and can be used to compute flux ratios over any range of negative reactivities. Several different values of prompt neutron lifetimes can also be used. It can be applied to any fuel for which the input parameters are available.

Subroutine RHOS

This subroutine is used as a tool to calculate single values of RHO when given a value of W, PNL, TB, II, and values for the arrays of DC and H. The end result is the parameter ROOS which is returned to the calling program. This program is called by the main program, FIRST, and HUNT.

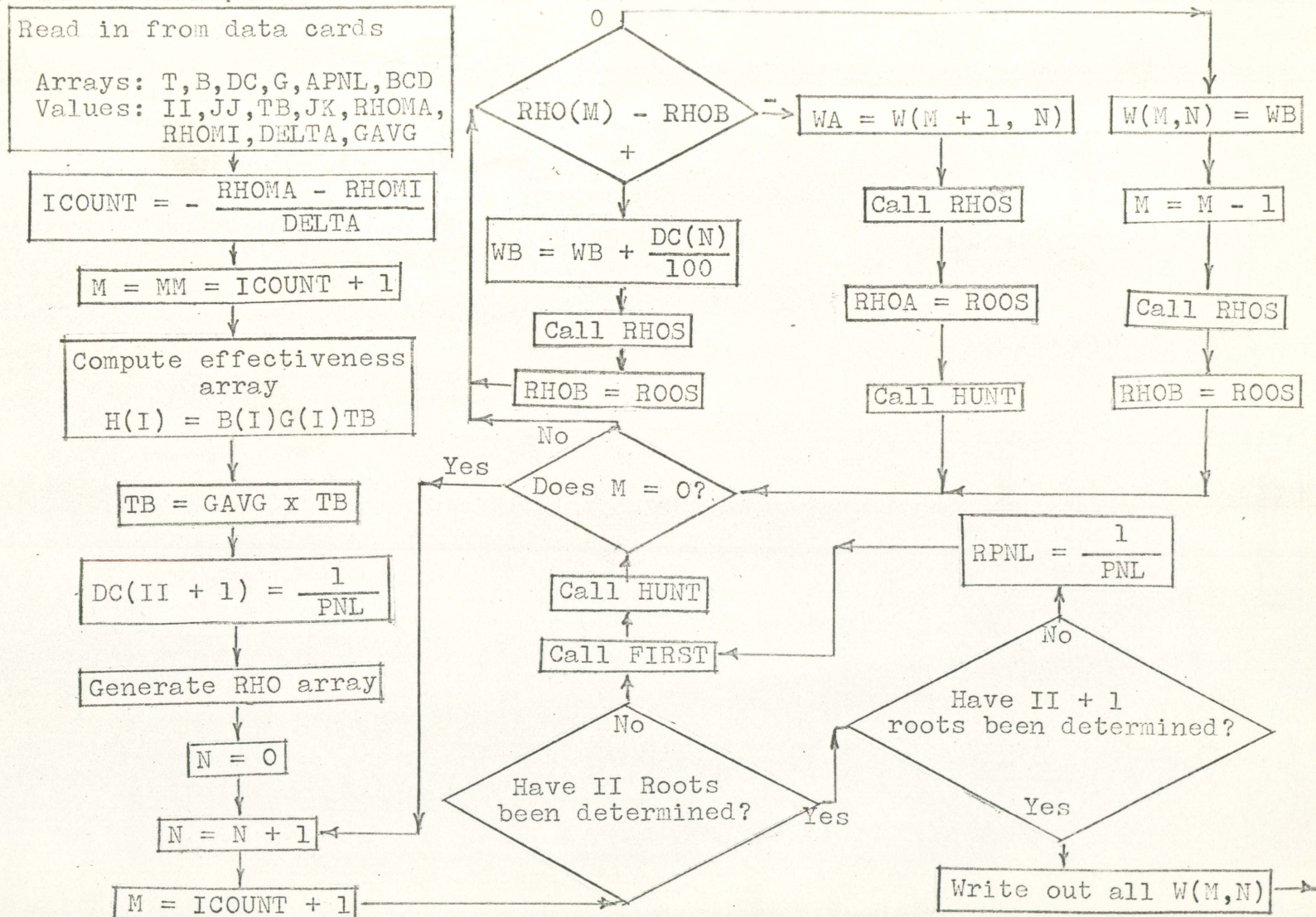


Figure 16. Flowsheet of main program

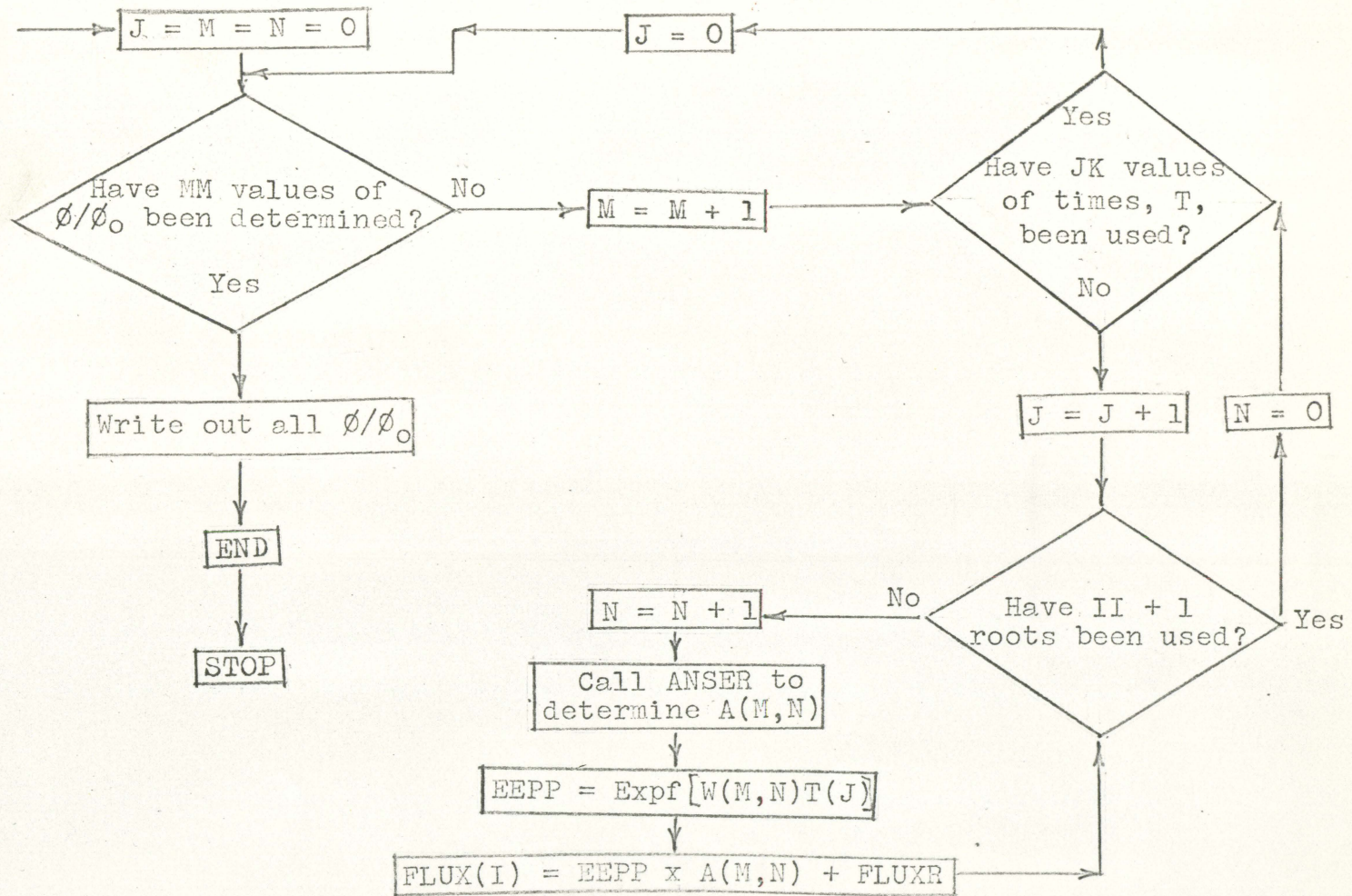


Figure 16. (continued)

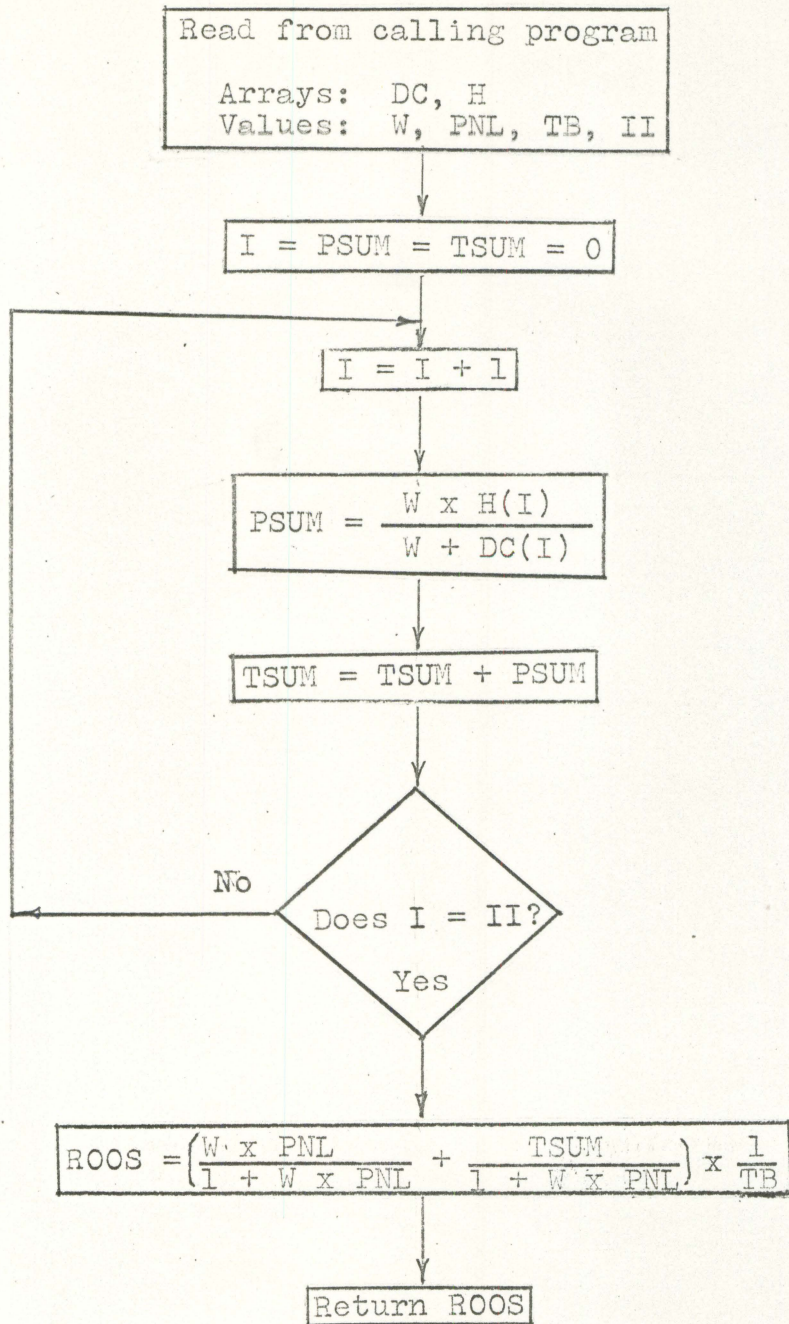


Figure 17. Flowsheet of subroutine RHOS

Subroutine FIRST

The purpose of this program is to determine the coordinates of two points of the reactivity versus β plot which will later initiate the iteration process. When the main program calls this subroutine, it designates which pole is to be considered. At this pole, AC, two points are determined, one which is slightly above and another which is slightly below the maximum value of negative reactivity, RHOMA. These coordinates are (WA,RHOA),(WB,RHOB). Because these points are selected by moving an incremental distance away from the pole, it is possible that this random value could correspond to RHOMA. In such a case, this value, W(M,N), would be returned to the main program as well as the coordinates of two lower points which satisfy the "above" and "below" stated above.

Subroutine HUNT

This program is the iteration process which begins with two points, A and B, whose coordinates are (RHOA,WA), (RHOB,WB) and through a process of extrapolation and checks determines a value of W which is within 10^{-5} of being an exact value for a particular value of the RHO array. The following figure and flow chart show the process used. The main program transfers the coordinates of the two points as well as the other values and arrays shown in the flow chart to the subprogram. An extrapolation is first made between A,B, and RHO(M) to determine WC. The value of rho, RHOC, which corresponds to WC is then determined by the subroutine

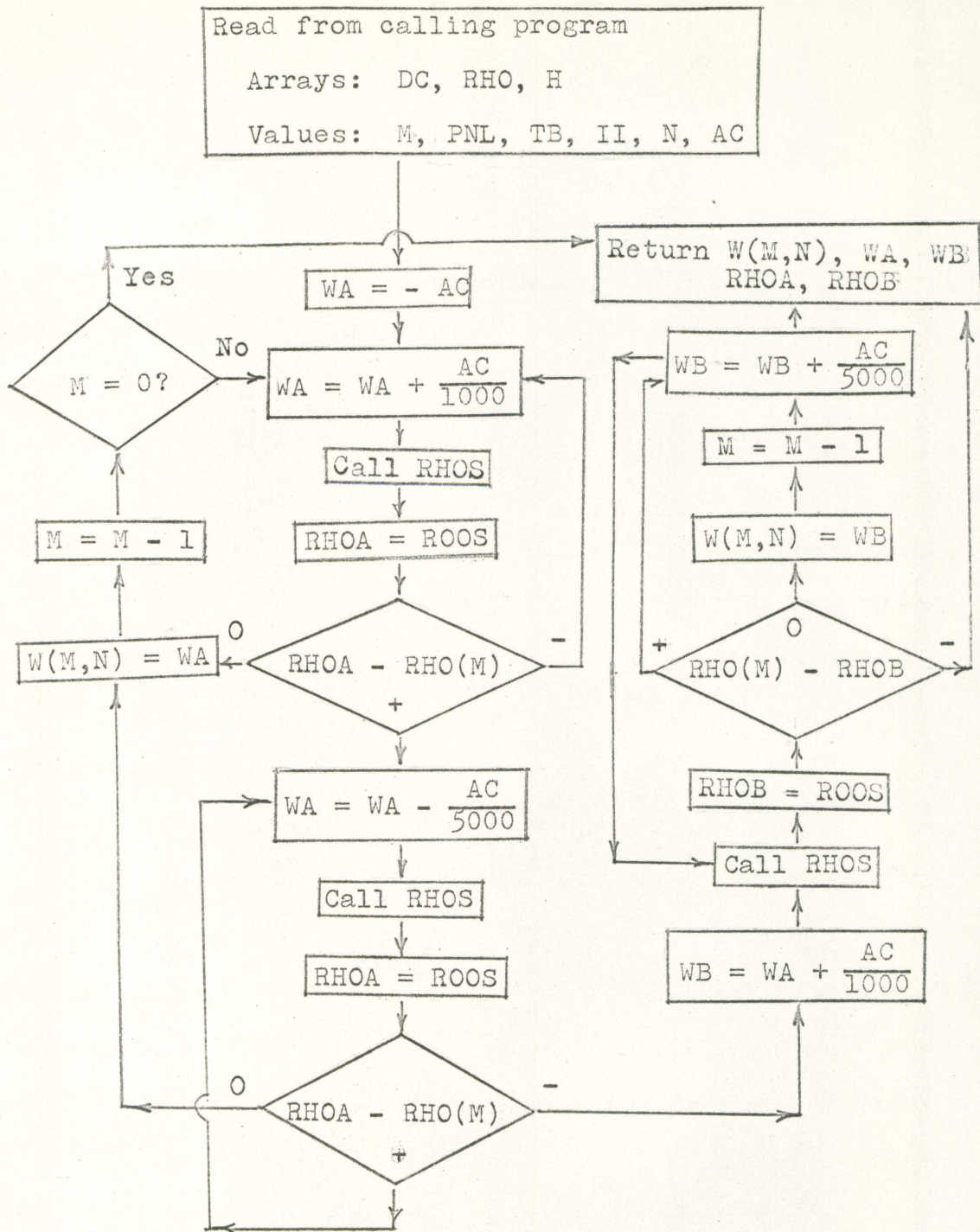


Figure 18. Flowsheet of subroutine FIRST

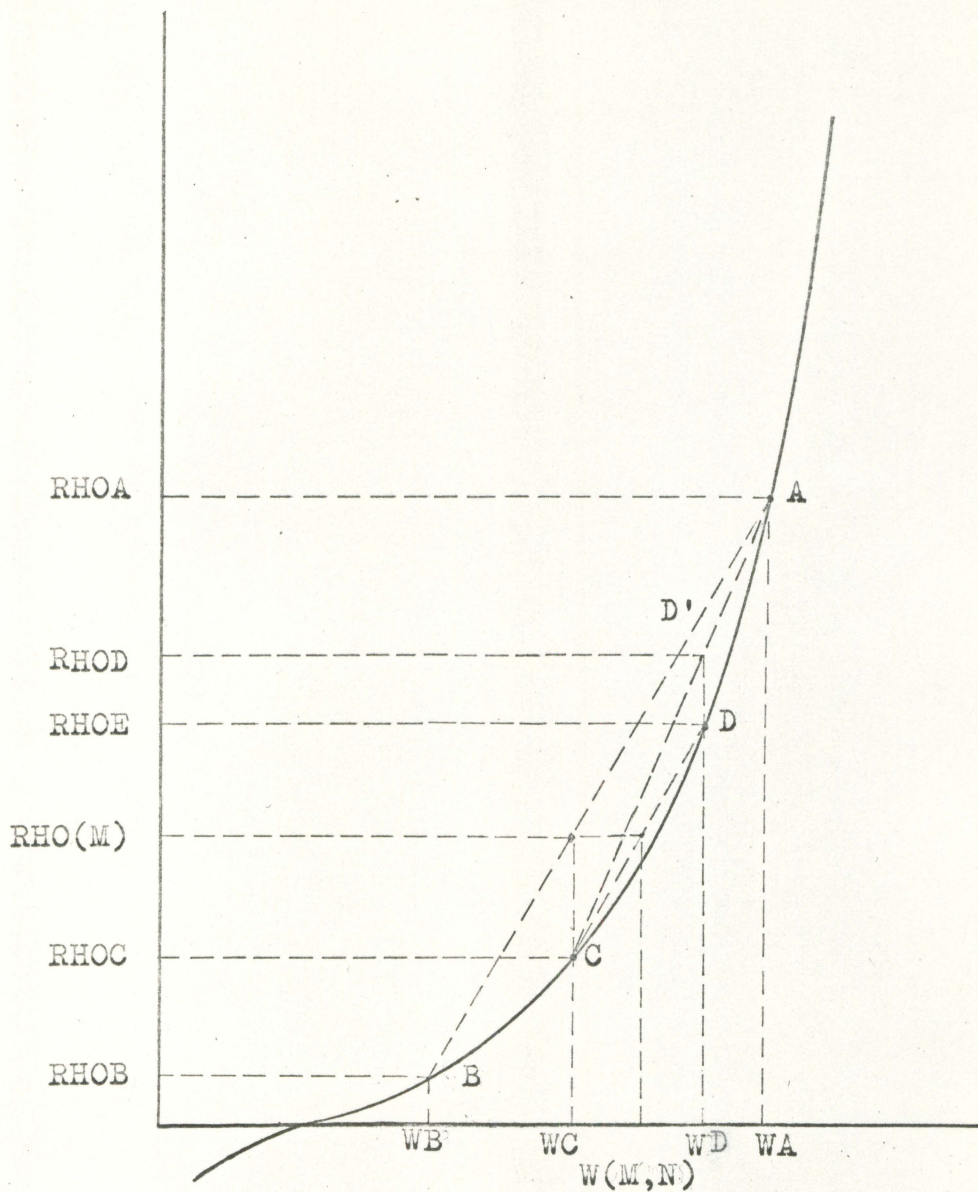


Figure 19. Curve used by iteration process in subroutine HUNT

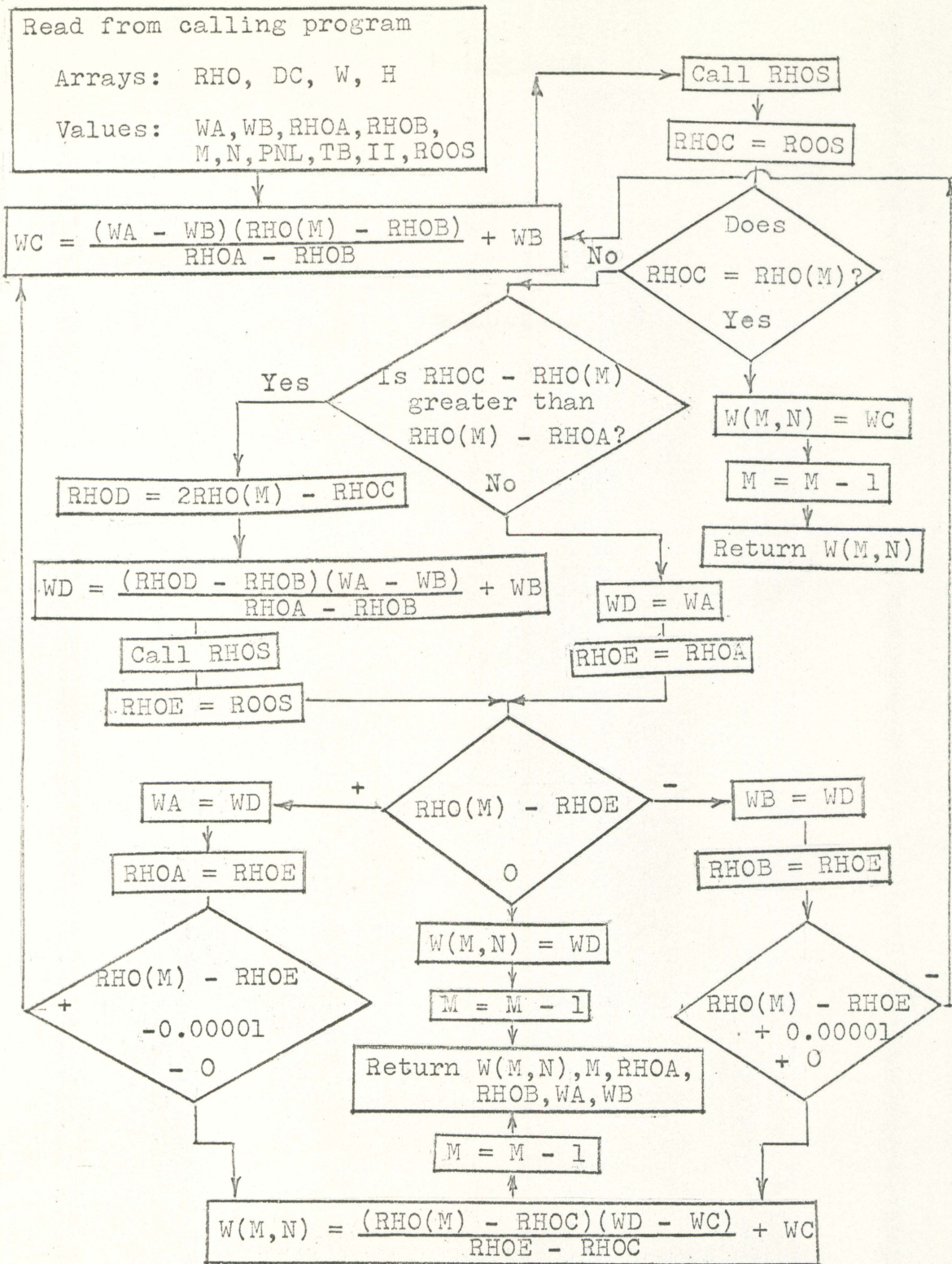


Figure 20. Flowsheet of subroutine HUNT

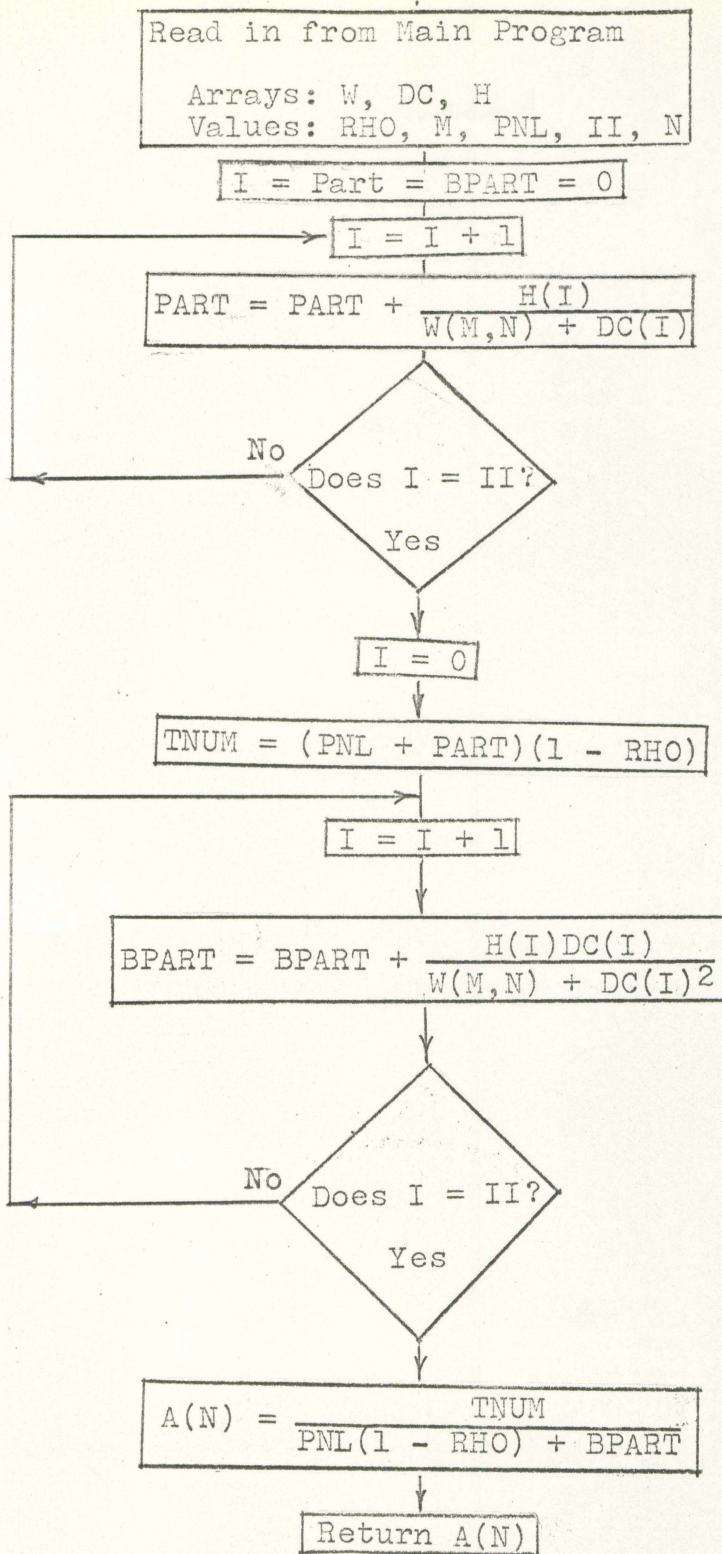


Figure 21. Flowsheet of subroutine ANSER

RHOS. A check is made to see if $RHO(N)$ is closer to $RHOA$ or $RHOC$. Should it be closer to $RHOC$, $RHOD$ is set to be at a distance of $RHO(N) - RHOC$ above $RHO(N)$ such that $RHO(N)$ lies midway between $RHOC$ and $RHOD$. $RHOE$ is then calculated by extrapolating between A , C , and $RHO(N)$ to find WD and then calling $RHOS$. Should $RHO(N)$ be closer to $RHOA$, point A is renamed point D . A check is then made to see if $RHOE$ is within 10^{-5} of $RHO(N)$. If it is, a final value of $W(N,N)$ is determined by extrapolating between points C and E . If this tolerance is not met, and if $RHO(N)$ is greater than $RHOE$, the interval is decreased by renaming point D as point E , or if $RHO(N)$ is less than $RHOE$, again the interval is decreased and point D is renamed point A . Should $RHO(N)$ exactly equal $RHOE$, $W(N,N)$ is set equal to WD and operation transferred to the end of the subprogram. In the case where the RHO value tolerance limit is not satisfied, the control is transferred to the initial extrapolation calculation with the decreased interval and the process repeated until tolerance has been obtained.

Subroutine ANSWER

This subroutine, like subroutine $RHOS$, serves simply as a means of calculating a single value, which in this case is an " A_j " term as given in Equation 4 and defined by Equation 5.

Negative Insertions into a Two Slab Reactor

The two slab computer solution for negative insertions of reactivity is a modified version of the preceding program and follows the same flow chart structure. New parameters and arrays have been introduced and are defined as follows.

Arrays:

ABA - A_{j1} coefficients

BAB - A_{j2} coefficients

FLR2 - Flux ratios in slab 2

AA - Coefficient matrix used in determining A_{j1}

BB - Coefficient matrix used in determining A_{j1}

SUM, XXP, DEN, are all work arrays defined by the program.

Values:

NRE - the number of roots expected in Equation 13

ALPHA - reactivity coupling coefficient

DK2 - reactivity of the second slab

TAU - the neutron delay time between slabs

TEST - a test value set upon completion of subroutines FIRST and SECOND; used to distinguish between poles located at $-\lambda_1$ and $-\lambda_1 + \Delta_1$

NP - the number of the pole being used in root evaluation

Subroutine SECOND is a modification of subroutine

FIRST and is used to calculate the initial iteration points at even numbered poles; subroutine FIRST calculates these points at odd numbered poles. Subroutine MATIN is used to solve the matrix of coefficients for the appropriate A_{j1} terms. This eliminates the need for subroutine ANSER. MATIN returns A_{j1} in array BB.


```

CALL .....FLAG.      I0147      JAWORSKI
FLAG  JOB,I0147,MAP
FLAG  FORT,MAIN
      DIMENSION APNL(9) ,G(7),H(7),FLUX (210,7),P(7),BCD(7),AFLX(210)
      DIMENSION B(7),DC(7),RHO(210),W(210,7),A(      7),T(20),FLR(20)
      READ INPUT TAPE 1,1,II,JJ,(APNL(I),I=1,JJ)
1     FORMAT(2I2,9E12.2)
2     FORMAT (E11.4)
      READ INPUT TAPE 1,2,(B(I),I=1,II)
      READ INPUT TAPE 1,2,(DC(I),I=1,II)
      READ INPUT TAPE 1,2,(G (I),I=1,II)
3     FORMAT(3F10.5)
      READ INPUT TAPE 1,3,RHOMA ,RHOMI ,DELTA
C     DETERMINE NUMBER OF VALUES OF RHO
      COUNT =(RHOMA -RHOMI )/DELTA
      ICOUN  =-COUNT
      II=II
      WA=WA
      WB=WB
      RHOA=RHOA
      RHOB=RHOB
      ROOS=ROOS
      PNL=PNL
      READ INPUT TAPE 1,41,TB,GAVG
41    FORMAT(2F10.6)
307   READ INPUT TAPE 1,308,JK
308   FORMAT (I5)
3071  READ INPUT TAPE 1,3081,(T(J),J=1,JK)
3081  FORMAT(F5.1)
      READ INPUT TAPE 1,700,(BCD(I),I=1,7)
700   FORMAT(7A5)
C     CHANGE ABUNDANCE RATIOS TO DELAYED NEUTRON FISSION FRACTION
      DO 431 I = 1,II
      B(I) = B(I)*TB
431   H(I) = B(I)*G(I)
      TB = TB*GAVG

```

Figure 22. Program for calculating one slab rod drop worths


```

411 DO 316 JM = 1, JJ
    PNL = APNL(JM)
    DC(II+1) = 1.00/PNL
199 N=0
    M=ICOUN + 1
    MM=ICOUN + 1
C   LOAD RHO ARRAY
    RHO(M)=RHOMA
    M=M-1
    DO 4 KM=1, ICOUN
    RHO(M)=RHO(M+1)+DELTA
    M=M-1
4   CONTINUE
200 M=ICOUN + 1
    N=N+1
2001 IF(N-(II+1))201,202,2021
201 O=DC(N)
    CALL FIRST (DC(1),      RHO(1),W(1,1),M,PNL,TB,WA,WB,II,RHOA,RHOB,
1N,O,H(1))
    CALL HUNT(WA,WB,RHOA,RHOB,RHO(1),M,N,      DC(1),PNL,TB,II,ROOS,
1W(1,1),H(1))
148 IF(M) 149,200,149
149 IF(RHO(M)-RHOB)150,1491,151
1491 W(M,N)=WB
    M=M-1
    GO TO 151
150 WA=W(M+1,N)
    CALL RHOS (WA,      DC(1),PNL,TB,II,ROOS,H(1))
    RHOA = ROOS
    CALL HUNT(W A      ,WB,RHOA      ,RHOB,RHO(1),M,N,      DC(1),PNL
1,TB,II,ROOS,W(1,1),H(1))
    GO TO 148
151 WB=WB+DC(N)/1000.0
    CALL RHOS(WB,      DC(1),PNL,TB,II,ROOS,H(1))
    RHOB=ROOS
    GO TO 148

```

Figure 22. (continued)


```

202  RPNL = 1.0/PNL
      CALL FIRST (DC(1),      RHO(1),W(1,1),M,PNL,TB,WA,WB,II,RHOA,RHOB,
1N,RPNL,H(1))
      CALL HUNT(WA,WB,RHOA,RHOB,RHO(1),M,N,      DC(1),PNL,TB,II,ROOS,
1W(1,1),H(1))
      GO TO 148
2021  CONTINUE
      WRITE OUTPUT TAPE 2,500,PNL
500   FORMAT(1H1,72H DETERMINATION OF THE TIME BEHAVIOR OF NUCLEAR DENSIT
1TY AND OF REACTIVITY,// 27H PROMPT NEUTRON LIFETIME...,E10.3)
      WRITE OUTPUT TAPE 2,5000,GAVG
5000  FORMAT(1H0,33HAVERAGE FISSION EFFECTIVENESS... ,F10.5)
      WRITE OUTPUT TAPE 2,502
502   FORMAT(1H0, 27H DELAYED NEUTRON PARAMETERS ,//79H GROUP,I      FRAC
1TION,B(I)      DECAY CONSTANT (/SEC)      FISSION EFFECTIVENESS )
      WRITE OUTPUT TAPE 2,503,(I,B(I),DC(I),G(I),I=1,II)
503   FORMAT(1H0,3X,I2,8X,E11.4,11X,E11.4,14X,E11.4)
      WRITE OUTPUT TAPE 2,504
504   FORMAT(1H1,113HREACTIVITY      W1      W2      W3
1      W4      W5      W6      W7      )
203   FORMAT(1H0,F8.4,7E15.4)
      III=II+1
      DO 205 M=1,MM
      WRITE OUTPUT TAPE 2,203, RHO(M), (W(M,N),N=1,III)
205   CONTINUE
C     END OF W PROGRAM
      WRITE OUTPUT TAPE 2,3082
3082  FORMAT(1H1,55X,12H FLUX RATIO ,///,50X,22HTIME AFTER ROD DROP )
      WRITE OUTPUT TAPE 2,3083,(T(J),J=1,JK)
3083  FORMAT(1H0,11HREACTIVITY , 7F15.4)
      DO 3111 M=1,MM
      DO 3111 J=1,JK
      FLUXR = 0
      DO 311 N=1,III
      IF(J-1)3101,3101,3104
3101  RHOR = RHO(M)*TB

```

Figure 22. (continued)


```

CALL ANSER(RHOR,          W(1,1),DC(1),A(1  ),M,PNL,II,N,H(1))
3104 X = W(M,N)*T(J)
      IF(100.+X)3111,3102,3102
3102 FLUXR=FLUXR + A( N)*EXPF(W(M,N)*T(J))
3119 FLR(J) = FLUXR
311  CONTINUE
      IF(JK-J)3111,3100,3111
3100 WRITE OUTPUT TAPE 2, 3112,RHO(M),(FLR(JT),JT=1,JK)
3112 FORMAT(1H0,F11.4,7E15.4)
      DO 3111 KJ = 1,JK
      FLUX(M,KJ) = FLR(KJ)
3111 CONTINUE
316  CONTINUE
318  CONTINUE
      END
      STOP
FLAG FORT RHOS
      SUBROUTINE RHOS(W,          DC          ,PNL,TB,II,ROOS,H)
      DIMENSION H(7), DC(7)
      JI = II
      PNL=PNL
      TB=TB
      ROOS=ROOS
      TSUM=0
      DO 6 I =1, JI
      PSUM = W*H(I)          /(W+DC(I))
      TSUM= TSUM + PSUM
6    CONTINUE
      ROOS=(W*PNL/(1.0+W*PNL)+TSUM/(1.0+PNL*W))/TB
7    RETURN
      END
FLAG FORT FIRST
      SUBROUTINE FIRST (DC          ,RHO          ,W          ,M,PNL,TB,WA,WB,II,RHO
1A,RHOB,N,AC,H)
      DIMENSION DC(7)          ,RHO(210),W(210,7),H(7)
      WA=-AC

```

Figure 22. (continued)


```

98     WA=WA+AC/1000.0
99     CALL RHOS(WA,      DC(1),PNL,TB,II,ROOS,H(1))
      RHOA =ROOS
      IF (RHOA-RHO(M)) 98,991,100
991    W(M,N)=WA
      M=M-1
      IF (M) 9911,1030,9911
9911   GO TO 98
100    WA=WA-AC/5000.0
      CALL RHOS(WA,      DC(1),PNL,TB,II,ROOS,H(1))
      RHOA = ROOS
      IF (RHOA-RHO(M)) 101,991,100
101    WB=WA+AC /1000.0
102    CALL RHOS(WB,      DC(1),PNL,TB,II,ROOS,H(1))
      RHOB=ROOS
      IF(RHO(M)-RHOB) 1031,1021,103
1021   W(M,N)=WB
      M=M-1
103    WB= WB+AC /5000.0
      GO TO 102
1030   CONTINUE
1031   RETURN
      AC=AC
      PNL=PNL
      TB=TB
      II=II
      ROOS=ROOS
      N=N
      END
FLAG  FORT  HUNT
      SUBROUTINE HUNT(WA,WB,RHOA,RHOB,RHO  ,M,N,      DC  , PNL,TB,II,
1ROOS,W,H)
      DIMENSION RHO(210),      DC(7),W(210,7),H(7)
104    WC=(WA-WB)*(RHO(M)-RHOB)/(RHOA-RHOB)+WB
      CALL RHOS(WC,      DC(1),PNL,TB,II,ROOS,H(1))
      RHOC=ROOS

```

Figure 22. (continued)


```

      IF(RHOC-RHO(M ))1042,1041,1042
1041  W(M,N)=WC
      GO TO 110
1042  IF(2.0*RHO(M)-RHOC-RHOA)106,106,105
105   RHOD=2.0*RHO(M)-RHOC
      GO TO 107
106   WD=WA
      RHOE=RHOA
      GO TO 1071
107   WD=(RHOD-RHOB)*(WA-WB)/(RHOA-RHOB)+WB
      CALL RHOS(WD,      DC(1),PNL,TB,II,ROOS,H(1))
      RHOE=ROOS
1071  IF(RHO(M )-RHOE) 108,1072,1090
1072  W(M,N)=WD
      GO TO 110
108   WB=WD
      RHOB=RHOE
      IF(RHO(M)-RHOE +0.00001) 104,1091,1091
1091  W(M,N) = WD
      GO TO 110
1090  WA=WD
      RHOA=RHOE
      IF(RHO(M) - RHOE -0.00001)1092,1092,104
1092  W(M,N)=(RHO(M)-RHOC)*(WD-WC)/(RHOE-RHOC)+WC
110   M=M-1
111   RETURN
      RHO(M) = RHO(M)
      RHOA = RHOA
      RHOB = RHOB
      WA = WA
      WB = WB
      WC=WC
      PNL=PNL
      TB=TB
      II=II
      N=N

```

Figure 22. (continued)


```

ROOS=ROOS
END
FLAG FORT ANSER
SUBROUTINE ANSER(RHO, W, DC, A, M, PNL, II, N, H)
DIMENSION W(210,7),DC(7),A(7),H(7)
PART = 0
BPART = 0
DO 300 I=1,II
300 PART = PART + H(I) / (W(M,N)+DC(I))
TNUM=(PNL+PART)*(1.0-RHO)
DO 301 I=1,II
301 BPART = BPART + H(I) * DC(I) / ((W(M,N) + DC(I))**2)
A( N)=TNUM/(PNL*(1.0 - RHO) + BPART)
RETURN
II=II
M=M
N=N
PNL=PNL
END

```

```

FLAG STAR
6 1 1.00E-04 4.00E-04 3.50E-04 4.00E-04
0.038E 00
0.213E 00
0.188E 00
0.407E 00
0.128E 00
0.026E 00
0.0127E 00
0.0317E 00
0.115E 00
0.311E 00
1.400E 00
3.870E 00
1.096E 00
1.028E 00
1.050E 00

```

Figure 22. (continued)

1.033E 00
1.000E 00
1.000E 00
-1.300 -0.0100 0.0100
0.650E-02 1.034E 00
7
30.0
60.0
120.0
180.0
240.0
300.0
360.0
NEG REACTIVITY (DOLLARS) FLUX RATIO

.....TOFOS

Figure 22. (continued)


```

CALL .....FLAG.      I0147      JAWORSKI
FLAG  JOB,I0147,MAP
FLAG  FORT,MAIN
      DIMENSION ABA( 75,15),BAB(75,15),FLR2(50,7)
      DIMENSION B(7),DC(7),RHO(105),W(105,15), T(20),FLR(20)
      DIMENSION APNL(9) ,G(7),H(7),P(7),BCD(7)
      DIMENSION AA(15,15),BB( 15,1),SUM(15),XXP(20),DEN(20)

C
C      SET NUMBER OF ROOTS EXPECTED
      NRE = 15
      READ (1,1)II,JJ,(APNL(I),I=1,JJ)
1     FORMAT(2I2,9E12.2)
2     FORMAT (E11.4)
      READ (1,2),(B(I),I=1,II)
      READ (1,2),(DC(I),I=1,II)
      READ(1,2),(G (I),I=1,II)
3     FORMAT(3F10.5)
      READ(1,3)RHOMA ,RHOMI ,DELTA

C
C      DETERMINE NUMBER OF VALUES TO BE IN RHO ARRAY
      COUNT =(RHOMA -RHOMI )/DELTA
      ICOUN  =-COUNT
      ALPHA = ALPHA
      DK2 = DK2
      DOL = DOL
      II=II
      PNL=PNL
      RHOA=RHOA
      RHOB=RHOB
      ROOS=ROOS
      TAU = TAU
      TEST = TEST
      WA=WA
      WB=WB
      READ INPUT TAPE 1,41,TB,GAVG,DK2,ALPHA,TAU
41    FORMAT(5E10.6)

```

Figure 23. Program for calculating two slab rod drop worths


```

307 READ (1,308) JK
308 FORMAT (I5)
3071 READ(1,3081),(T(J),J=1,JK)
3081 FORMAT(F5.1)
      READ(1,700),(BCD(I),I=1,7)
700  FORMAT(7A5)
C
C      CONVERT ABUNDANCE RATIOS TO DELAYED NEUTRON FISSION FRACTION
      DO 431 I = 1,II
      B(I) = B(I)*TB
431  H(I) = B(I)*G(I)
      TB = TB*GAVG
C
C      COMPUTE DOLLAR VALUE FOR TWO SLAB SYSTEM AT INITIAL CRITICAL PT
      SDOL = 1.0 - TB
      AK1P = ((ALPHA**2)/((DK2 + 1.0)*SDOL - 1.0) + 1.0)/SDOL
      DOL = AK1P - ALPHA**2/DK2
      DO 316 JM = 1,JJ
411  PNL = APNL(JM)
      TEST = 0.0
199  N=0
      M=ICOUN + 1
      MM=ICOUN + 1
      RHO(M)=RHOMA
      M=M-1
C
C      FILL RHO ARRAY
      DO 4 KM=1,ICOUN
      RHO(M)=RHO(M+1)+DELTA
      M=M-1
4   CONTINUE
200  M=ICOUN +1
      N=N+1
      IF(N-NRE-1) 2222,2005,2222
2222 NP = (N-1)/2 + 1
2001 IF(NP-(II+1))201,202,2021

```

Figure 23. (continued)


```

201  Z = DC(NP)
C
C      DETERMINE IF ROOT TO BE CALCULATED IS WITH AN EVEN OR ODD POLE
      IF (TEST) 2112,2111,2112
2111  CALL FIRST (DC(1),      RHO(1),W(1,1),M,PNL,TB,WA,WB,II,RHOA,RHOB,
1N,Z,H(1),DK2,TAU,ALPHA,TEST,DOL)
21111 CALL HUNT(WA,WB,RHOA,RHOB,RHO(1),M,N,      DC(1),PNL,TB,II,ROOS,
1W(1,1),H(1),DK2,TAU,ALPHA,NP,DOL)
      GO TO 148
2112  CALL SECND (DC(1),      RHO(1),W(1,1),M,PNL,TB,WA,WB,II,RHOA,RHOB,
1N,Z,H(1),DK2,TAU,ALPHA,TEST,DOL)
      GO TO 21111
148   IF(M) 149,200,149
149   IF(RHO(M)-RHOB)150,1491,151
1491  W(M,N)=WB
      M=M-1
      GO TO 151
150   WA=W(M+1,N)
      CALL RHOS (WA,      DC(1),PNL,TB,II,ROOS,H(1),DK2,TAU,ALPHA,DOL)
      RHOA = ROOS
      CALL HUNT(WA,WB,RHOA,RHOB,RHO(1),M,N,      DC(1),PNL,TB,II,ROOS,
1W(1,1),H(1),DK2,TAU,ALPHA,NP,DOL)
      GO TO 148
151   WB = WB + DC(NP)/1000.0
1511  CALL RHOS(WB,      DC(1),PNL,TB,II,ROOS,H(1),DK2,TAU,ALPHA,DOL)
      RHOB=ROOS
      IF(RHOB) 148,148,1485
1485  WB = WB - DC(NP)/4100.0
      GO TO 1511
202   IF(N-14) 2002,2003,2021
2002  Z = 100.0
      DC(7) = Z
      GO TO 2004
2003  Z = 500.0
      DC(7) = Z
2004  CALL FIRST (DC(1),      RHO(1),W(1,1),M,PNL,TB,WA,WB,II,RHOA,RHOB,

```

Figure 23. (continued)


```

      1N,Z,H(1),DK2,TAU,ALPHA,TEST,DOL)
20041 CALL HUNT(WA,WB,RHOA,RHOB,RHO(1),M,N,      DC(1),PNL,TB,II,ROOS,
      1W(1,1),H(1),DK2,TAU,ALPHA,NP,DOL)
      GO TO 148
2021  DC(7) = 5000.0
      Z = 26500.0
      CALL SECND (DC(1),      RHO(1),W(1,1),M,PNL,TB,WB,WA,II,RHOB,RHOA,
      1N,Z,H(1),DK2,TAU,ALPHA,TEST,DOL)
      CALL HUNT(WB,WA,RHOB,RHOA,RHO(1),M,N,      DC(1),PNL,TB,II,ROOS,
      1W(1,1),H(1),DK2,TAU,ALPHA,NP,DOL)
7148  IF(M) 7149, 200,7149
7149  IF(RHO(M) - RHOA)7150,71491,7151
71491  W(M,N) = WA
      M = M - 1
      GO TO 7151
7150  WB = W(M+1,N)
      CALL RHOS(WB,      DC(1),PNL,TB,II,ROOS,H(1),DK2,TAU,ALPHA,DOL)
      RHOB = ROOS
      CALL HUNT(WB,WA,RHOB,RHOA,RHO(1),M,N,      DC(1),PNL,TB,II,ROOS,
      1W(1,1),H(1),DK2,TAU,ALPHA,NP,DOL)
C      PROGRAM COULD HANG HERE IF CURVE IS TOO STEEP
C      FOLLOWING STATEMENTS WERE USED TO FORCE PROGRAM TO GO
C      CALL DUMP AAA
C      IF(M-25) 71501,71501,71481
C71501 DO 71502 I=1,25
C      M = MM - 20 - I
C      W(M,N) = W(26,15)
C71502 CONTINUE
C      GO TO 200
C 71481 GO TO 7148
7151  WA = WA - DC(7)/1000.0
71511 CALL RHOS(WA,      DC(1),PNL,TB,II,ROOS,H(1),DK2,TAU,ALPHA,DOL)
      RHOA = ROOS
      IF(RHOA) 7148,7148,71485
71485 WA = WA + DC(7)/6100.0
      GO TO 71511

```

Figure 23. (continued)


```

2005 CONTINUE
      WRITE OUTPUT TAPE 2,500,PNL
500  FORMAT(1H1,72H DETERMINATION OF THE TIME BEHAVIOR OF NUCLEAR DENSIT
      Y AND OF REACTIVITY, // 27H PROMPT NEUTRON LIFETIME...,E10.3)
      WRITE OUTPUT TAPE 2,5000,GAVG
5000 FORMAT(1H0,33HAVERAGE FISSION EFFECTIVENESS... ,F10.5)
      WRITE OUTPUT TAPE 2,502
502  FORMAT(1H0, 27H DELAYED NEUTRON PARAMETERS ,//79H GROUP,I      FRAC
      ITION,B(I)      DECAY CONSTANT (/SEC)      FISSION EFFECTIVENESS )
      WRITE OUTPUT TAPE 2,503,(I,B(I),DC(I),G(I),I=1,II)
503  FORMAT(1H0,3X,I2,8X,E11.4,11X,E11.4,14X,E11.4)
      WRITE OUTPUT TAPE 2,504
504  FORMAT(1H1,113HREACTIVITY      W1      W2      W3
      1      W4      W5      W6      W7      )
203  FORMAT(1H0,F8.4,7E15.8)
2030 FORMAT(11X,7E15.8)
      III=II+1
      DO 205 M=1,MM
      WRITE OUTPUT TAPE 2,203, RHO(M), (W(M,N),N=1,III)
      WRITE OUTPUT TAPE 2,2030, (W(M,N),N=8,14)
      WRITE (2,2030) W(M,15)
205  CONTINUE
C
C      END OF W PROGRAM
C
      AK2 = DK2 + 1.0
      WRITE OUTPUT TAPE 2,3082
3082 FORMAT(1H1,55X,12H FLUX RATIO ,///,50X,22HTIME AFTER ROD DROP )
      WRITE OUTPUT TAPE 2,3083,(T(J),J=1,JK)
3083 FORMAT(1H0,11HREACTIVITY , 7F15.4)
      DO 3111 M=1,MM
3101 CONTINUE
C
C      LOADING OF A1 COEFFICIENT MATRIX
      NMN = NRE
      DO 851 L = 1,NMN

```

Figure 23. (continued)


```

AA(1,L) = 1.0
851 CONTINUE
DO 860 NJN = 1,NMN
SUM(NJN) = 0.0
DO 860 I = 1,II
SUM(NJN) = SUM(NJN) + H(I)*W(M,NJN)/(W(M,NJN) + DC(I))
860 CONTINUE
BB(1,1) = 1.0
DO 852 L = 1,NMN
XXP(L) = ALPHA*EXPF(-W(M,L)*TAU)
DEN(L) = PNL*W(M,L) - DK2 + AK2*SUM(L)
AA(2,L) = XXP(L)/DEN(L)
852 CONTINUE
BB(2,1) = -ALPHA/DK2
DO 854 I=3,8
DO 853 L = 1,NMN
AA(I,L) = 1.0/(W(M,L) + DC(I-2))
853 CONTINUE
BB(I,1) = 1.0/DC(I -2)
854 CONTINUE
DO 856 I = 9,14
DO 855 L = 1,NMN
AA(I,L) = XXP(L)/(DEN(L)*(W(M,L) + DC(I-8)))
855 CONTINUE
BB(I,1) = -ALPHA/(DK2*DC(I-8))
856 CONTINUE
IF(NRE-15) 858,8571,858
8571 DO 857 L = 1,NMN
AA(15,L) = AA(2,L)*W(M,L)
857 CONTINUE
BB(15,1) = 0.0
858 MNM = 1
CALL MATIN(AA(1,1),NMN,BB(1,1),MNM,DETER)
DETER = DETER

C
C COMPUTE A2 COEFFICIENT FOR SECOND SLAB AND STORE A1 COEF.

```

Figure 23. (continued)


```

C      COEFFICIENTS FOR SLAB 1 ARE RETURNED FROM MATIN IN BB ARRAY
      DO 859 L=1,NMN
      ABA(M,L) = BB(L,1)
      BAB(M,L) = XXP(L)*BB(L,1)/DEN(L)
859   CONTINUE
      IF(BB(1,1)) 809,903,809

C
C      DETERMINE FLUX RATIOS FOR TIMES IN T ARRAY
809   DO 3111 J=1,JK
      FLUXR = 0
      FL2XR = 0.0
      DO 311 N=1,NMN
3104  X = W(M,N)*T(J)
      IF(100.0+X)311 ,3102,3102
3102  X = EXPF(X)
      FLUXR=FLUXR +BB(N,1)*X
      FL2XR = FL2XR + BAB(M,N)*X
      FLR2(M,J) = FL2XR
3119  FLR(J) = FLUXR
311   CONTINUE
      IF(JK-J)3111,3100,3111
3100  WRITE OUTPUT TAPE 2,3112,RHO(M),(FLR(JT),JT=1,JK)
3112  FORMAT(1H0,F11.4,7E15.4)
3111  CONTINUE
      WRITE OUTPUT TAPE 2,30821
30821 FORMAT(1H1,45X,26H FLUX RATIO IN SECOND SLAB,///,50X,19HTIME AFTER
      1 ROD DROP)
      WRITE OUTPUT TAPE 2,30831,(T(J),J=1,JK)
30831 FORMAT(1H0,11HREACTIVITY , 7F15.4)
31121 FORMAT(1H0,F11.4,7E15.4)
      DO 316 M =1,MM
      WRITE(2,31121), RHO(M),(FLR2(M,J),J=1,JK)
316   CONTINUE
      CALL DUMP LLL
318   CONTINUE
903   CONTINUE

```

Figure 23. (continued)


```

      END
      STOP
FLAG FORT RHOS
      SUBROUTINE RHOS(W,DC,PNL,TB,II,ROOS,H,DK2,TAU,ALPHA,DOL)
      DIMENSION H(7), DC(7)
      AK2 = DK2 + 1.0
      SUM = 0.0
      DO 5 I = 1,II
      SUM = H(I)/(DC(I) + W) + SUM
5      CONTINUE
      A = DK2 - W*PNL - W*SUM*AK2
      X = -2.0* W*TAU
      ANUM = (ALPHA**2)*EXPF(X) + (W*PNL + 1.0)*A
      DEN = A*(1.0 - W*SUM)
      DK1 = ANUM/DEN - 1.0 - ALPHA**2/DK2
      ROOS = DK1/((DK1+1.0)*DOL)
      RETURN
      ALPHA = ALPHA
      DK2 = DK2
      DOL = DOL
      II = II
      PNL=PNL
      ROOS=ROOS
      TAU = TAU
      TB=TB
      END
FLAG FORT FIRST
      SUBROUTINE FIRST (DC ,RHO ,W ,M,PNL,TB,WA,WB,II,RHO
1A,RHOB,N,AC,H ,DK2,TAU,ALPHA,TEST,DOL)
      DIMENSION DC(7) ,RHO(105),W(105,15),H(7)
97      WA=-AC
98      WA=WA+AC/4.0
99      CALL RHOS(WA, DC(1),PNL,TB,II,ROOS,H(1),DK2,TAU,ALPHA,DOL)
      RHOA =ROOS
      IF(RHOA) 999,999,998
998      WA = WA - AC/200.0

```

Figure 23. (continued)


```

GO TO 99
999 IF (RHOA-RHO(M)) 101,991,100
991 W(M,N)=WA
M=M-1
IF (M) 9911,1030,9911
9911 GO TO 98
100 WA=WA-AC/200.0
CALL RHOS(WA, DC(1),PNL,TB,II,ROOS,H(1),DK2,TAU,ALPHA,DOL)
RHOA = ROOS
IF (RHOA-RHO(M)) 101,991,100
101 WB=WA+AC /100.0
102 CALL RHOS(WB, DC(1),PNL,TB,II,ROOS,H(1),DK2,TAU,ALPHA,DOL)
RHOB=ROOS
IF(RHOB) 9400,9400,9401
9401 WB = WB - AC/500.
GO TO 102
9400 IF(RHO(M)-RHOB) 1031,1021,103
1021 W(M,N)=WB
M=M-1
103 WB = WB + AC/200.0
GO TO 102
1030 CONTINUE
1031 TEST = 1.0
RETURN
AC=AC
ALPHA = ALPHA
DK2 = DK2
DOL = DOL
II=II
M = M
N=N
PNL=PNL
ROOS=ROOS
TAU = TAU
TB=TB
TEST = TEST

```

Figure 23. (continued)


```

END
FLAG FORT SECND
SUBROUTINE SECND (DC ,RHO ,W ,M,PNL,TB,WA,WB,II,RHO
1A,RHOB,N,AC,H ,DK2,TAU,ALPHA,TEST,DOL)
DIMENSION DC(7) ,RHO(105),W(105,15),H(7)
WA=-AC
IF(N-15) 98,97,98
97 AC = -AC/2.
98 WA=WA+AC/500.0
99 CALL RHOS(WA, DC(1),PNL,TB,II,ROOS,H(1),DK2,TAU,ALPHA,DOL)
RHOA =ROOS
IF(RHOA) 999,999,998
998 WA = WA - AC/1100.0
GO TO 99
999 IF (RHOA-RHO(M)) 101,991,100
991 W(M,N)=WA
M=M-1
IF (M) 9911,1030,9911
9911 GO TO 98
100 WA=WA-AC/3400.0
CALL RHOS(WA, DC(1),PNL,TB,II,ROOS,H(1),DK2,TAU,ALPHA,DOL)
RHOA = ROOS
IF (RHOA-RHO(M)) 101,991,100
101 WB=WA+AC /3000.0
102 CALL RHOS(WB, DC(1),PNL,TB,II,ROOS,H(1),DK2,TAU,ALPHA,DOL)
RHOB=ROOS
IF(RHOB) 9400,9400,9401
9401 WB = WB - AC/7000.0
GO TO 102
9400 IF(RHO(M)-RHOB) 1031,1021,103
1021 W(M,N)=WB
M=M-1
103 WB = WB + AC/2500.0
GO TO 102
1030 CONTINUE
1031 TEST = 0.0

```

Figure 23. (continued)


```

1033 RETURN
      AC=AC
      ALPHA = ALPHA
      DK2 = DK2
      DOL = DOL
      II=II
      M = M
      N=N
      PNL=PNL
      ROOS=ROOS
      TAU = TAU
      TB=TB
      TEST = TEST
      END
FLAG FORT HUNT
      SUBROUTINE HUNT(WA,WB,RHOA,RHOB,RHO ,M,N, DC , PNL,TB,II,
1ROOS,W,H,DK2,TAU,ALPHA,NP,DOL)
      DIMENSION DC(7) ,RHO(105),W(105,15),H(7)
104 WC=(WA-WB)*(RHO(M)-RHOB)/(RHOA-RHOB)+WB
      IF(WC-WB) 1052,1051,1052
1052 IF(WC-WA) 1053,1051,1053
1051 W(M,N) = WA
      GO TO 110
1053 CALL RHOS(WC, DC(1),PNL,TB,II,ROOS,H(1),DK2,TAU,ALPHA,DOL)
      RHOC=ROOS
      IF(RHOC-RHO(M ))1042,1041,1042
1041 W(M,N)=WC
      GO TO 110
1042 IF(2.0*RHO(M)-RHOC-RHOA)106,106,105
105 RHOD=2.0*RHO(M)-RHOC
      GO TO 107
106 RHOD = 2.0*RHO(M) - RHOA
107 WD=(RHOD-RHOC)*(WA-WC)/(RHOA-RHOC)+WC
      IF(WD-WB) 1073,1041,1073
1073 CALL RHOS(WD, DC(1),PNL,TB,II,ROOS,H(1),DK2,TAU,ALPHA,DOL)
      RHOE=ROOS

```

Figure 23. (continued)


```

1071 IF(RHO(M)-RHOE) 108,1072,1090
1072 W(M,N)=WD
      GO TO 110
108   WB=WD
      RHOB=RHOE
      IF(RHO(M)-RHOE +0.0001 ) 104,1091,1091
1091  W(M,N) = WD
      GO TO 110
1090  WA=WD
      RHOA=RHOE
      WB = WC
      RHOB = RHOC
      IF(RHO(M) - RHOE -0.0001 )1092,1092,104
1092  W(M,N)=(RHO(M)-RHOC)*(WD-WC)/(RHOE-RHOC)+WC
110   M=M-1
111   RETURN
      ALPHA = ALPHA
      DK2 = DK2
      DOL = DOL
      II=II
      M = M
      N=N
      NP = NP
      PNL=PNL
      RHO(M) = RHO(M)
      RHOA = RHOA
      RHOB = RHOB
      ROOS=ROOS
      TAU = TAU
      TB=TB
      WA = WA
      WB = WB
      WC=WC
      END
FLAG FORT  MATIN
      SUBROUTINE MATIN (A,N,B,M,DETER)

```

Figure 23. (continued)

C	MATRIX INVERSION WITH ACCOMPANYING SOLUTION OF LINEAR EQUATIONS	ANF40201
C		
	DIMENSION IPIVO(15),A(15, 15),B(15,1),INDEX(15,2),PIVOT(15)	F4020005
	EQUIVALENCE (IROW,JROW), (ICOLU,JCOLU), (AMAX, T, SWAP)	
C		
C	INITIALIZATION	F4020009
C		F4020010
	10 DETER=1.0	F4020011
	15 DO 20 J=1,N	F4020012
	20 IPIVO(J)=0	F4020013
	30 DO 550 I=1,N	F4020014
C		F4020015
C	SEARCH FOR PIVOT ELEMENT	F4020016
C		F4020017
	40 AMAX=0.0	F4020018
	45 DO 105 J=1,N	F4020019
	50 IF (IPIVO(J)-1) 60, 105, 60	F4020020
	60 DO 100 K=1,N	F4020021
	70 IF (IPIVO(K)-1) 80, 100, 740	F4020022
	80 IF (ABSF(AMAX)-ABSF(A(J,K))) 85, 100, 100	F4020023
	85 IROW=J	F4020024
	90 ICOLU=K	F4020025
	95 AMAX=A(J,K)	F4020026
	100 CONTINUE	F4020027
	105 CONTINUE	F4020028
	110 IPIVO(ICOLU)=IPIVO(ICOLU)+1	F4020029
C		F4020030
C	INTERCHANGE ROWS TO PUT PIVOT ELEMENT ON DIAGONAL	F4020031
C		F4020032
	130 IF (IROW-ICOLU) 140, 260, 140	F4020033
	140 DETER=-DETER	F4020034
	150 DO 200 L=1,N	F4020035
	160 SWAP=A(IROW,L)	F4020036
	170 A(IROW,L)=A(ICOLU,L)	F4020037
	200 A(ICOLU,L)=SWAP	F4020038
	205 IF(M) 260, 260, 210	F4020039

Figure 23. (continued)

210 DO 250 L=1, M	F4020040
220 SWAP=B(IROW,L)	F4020041
230 B(IROW,L)=B(ICOLU,L)	F4020042
250 B(ICOLU,L)=SWAP	F4020043
260 INDEX(I,1)=IROW	
270 INDEX(I,2)=ICOLU	F4020045
310 PIVOT(I)=A(ICOLU,ICOLU)	F4020046
320 DETER=DETER*PIVOT(I)	F4020047
C	F4020048
C DIVIDE PIVOT ROW BY PIVOT ELEMENT	F4020049
C	F4020050
330 A(ICOLU,ICOLU)=1.0	F4020051
340 DO 350 L=1,N	F4020052
350 A(ICOLU,L)=A(ICOLU,L)/PIVOT(I)	F4020053
355 IF(M) 380, 380, 360	F4020054
360 DO 370 L=1,M	F4020055
370 B(ICOLU,L)=B(ICOLU,L)/PIVOT(I)	F4020056
C	F4020057
C REDUCE NON-PIVOT ROWS	F4020058
C	F4020059
380 DO 550 L1=1,N	F4020060
390 IF(L1-ICOLU) 400, 550, 400	F4020061
400 T=A(L1,ICOLU)	F4020062
420 A(L1,ICOLU)=0.0	F4020063
430 DO 450 L=1,N	F4020064
450 A(L1,L)=A(L1,L)-A(ICOLU,L)*T	F4020065
455 IF(M) 550, 550, 460	F4020066
460 DO 500 L=1,M	F4020067
500 B(L1,L)=B(L1,L)-B(ICOLU,L)*T	F4020068
550 CONTINUE	F4020069
C	F4020070
C INTERCHANGE COLUMNS	F4020071
C	F4020072
600 DO 710 I=1,N	F4020073
610 L=N+1-I	F4020074
620 IF (INDEX(L,1)-INDEX(L,2)) 630, 710, 630	F4020075

Figure 23. (continued)


```

630 JROW=INDEX(L,1)
640 JCOLU=INDEX(L,2)
650 DO 705 K=1,N
660 SWAP=A(K,JROW)
670 A(K,JROW)=A(K,JCOLU)
700 A(K,JCOLU)=SWAP
705 CONTINUE
710 CONTINUE
740 RETURN
      END

```

```

F4020076
F4020077
F4020078
F4020079
F4020080
F4020081
F4020082
F4020083
F4020084

```

```

FLAG STAR
6 1      1.00E-04      4.00E-04      3.50E-04      4.00E-04
0.038E 00
0.213E 00
0.188E 00
0.407E 00
0.128E 00
0.026E 00
0.0127E 00
0.0317E 00
0.115E 00
0.311E 00
1.400E 00
3.870E 00
1.096E 00
1.028E 00
1.050E 00
1.033E 00
1.000E 00
1.000E 00
      -1.000      -0.1000      0.0200
0.650E-02 1.034E 00-0.916E-02 0.100E-01 0.210E-03
7
30.0
60.0
120.0

```

Figure 23. (continued)

180.0
240.0
300.0
360.0
NEG REACTIVITY (DOLLARS) FLUX RATIO

.....TOFOS

Figure 23. (continued)

APPENDIX B

Development of the Kinetic Equations
for a Two Slab Core

The methods used to develop Equation 9 which relates the reactivity of each slab and " ω " are presented here.

For slab 1, the neutron density equation is

$$\frac{dn_1}{dt} = \frac{\delta K_1}{l} n_1 - \frac{K_1 \gamma_{avg} \beta}{l} n_1 + \sum_{i=1}^M \gamma_i \lambda_i^{-1} C_{i1} + \frac{\alpha}{l} n_2(t - \tau) \quad (1B)$$

Because the reactor exhibits a single exponential period at sometime after a change in reactivity, it can safely be assumed that the neutron density equation follows the form such that

$$n(t) = n_0 e^{\omega t} \quad (2B)$$

$$n_1(t) = n_{10} e^{\omega t} \quad (3B)$$

$$n_2(t) = n_{20} e^{\omega t} \quad (4B)$$

$$n_2(t - \tau) = n_{20} e^{\omega(t - \tau)}. \quad (5B)$$

Also it is assumed that

$$C_{i1} = C_{i10} e^{\omega t} \quad (6B)$$

$$C_{i2} = C_{i20} e^{\omega t}. \quad (7B)$$

Placing Equations 3B, 5B and 6B into 1B yields

$$n_1 \omega = \frac{\delta K_1}{l} n_1 - \frac{K_1 \gamma_{avg} \beta}{l} n_1 + \sum_{i=1}^M \gamma_i \lambda_i^{-1} C_{i1} + \frac{\alpha n_2}{l} e^{-\omega \tau}. \quad (8B)$$

Similarly for slab 2,

$$n_2 \omega = \frac{\delta K_2}{l} n_2 - \frac{K_2 \gamma_{avg} \beta}{l} n_2 + \sum_{i=1}^M \gamma_i \lambda_i^{-1} C_{i2} + \frac{\alpha n_1}{l} e^{-\omega \tau}. \quad (9B)$$

The precursor concentration term, C_1 , may be eliminated by using Equations 6B and 7B and the expression

$$\frac{dC_1}{dt} = \frac{K\beta_1}{l} n - \lambda_1 C_1. \quad (10B)$$

For slab 1, this result is

$$\begin{aligned} \omega C_{11} &= \frac{K_1\beta_1}{l} n_1 - \lambda_1 C_{11} \\ C_{11} &= \frac{K_1\beta_1}{l(\omega + \lambda_1)} n_1. \end{aligned} \quad (11B)$$

A similar expression exists for slab 2.

Placing Equation 11B into Equation 8B and collecting terms yields

$$\left(\frac{\delta K_1}{l} - \omega - \frac{K_1}{l} \sum_{i=1}^M \frac{\gamma_i \beta_i \omega}{\omega + \lambda_i} \right) n_1 + \frac{\alpha}{l} n_2 e^{-\omega \tau} = 0. \quad (12B)$$

For slab 2, this equation is

$$\frac{\alpha}{l} n_1 e^{-\omega \tau} + \left(\frac{\delta K_2}{l} - \omega - \frac{K_2}{l} \sum_{i=1}^M \frac{\gamma_i \beta_i \omega}{\omega + \lambda_i} \right) n_2 = 0. \quad (13B)$$

If n_1 and n_2 are not to be trivial solutions, the determinant of the coefficients on n_1 and n_2 in Equations 12B and 13B should equal zero. Thus,

$$\begin{vmatrix} \frac{\delta K_1}{l} - \omega - \frac{K_1}{l} \sum_{i=1}^M \frac{\gamma_i \beta_i \omega}{\omega + \lambda_i} & \frac{\alpha}{l} e^{-\omega \tau} \\ \frac{\alpha}{l} e^{-\omega \tau} & \frac{\delta K_2}{l} - \omega - \frac{K_2}{l} \sum_{i=1}^M \frac{\gamma_i \beta_i \omega}{\omega + \lambda_i} \end{vmatrix} = 0. \quad (14B)$$

APPENDIX C

Matrix Derivation

The assumptions and equations used in setting up a fifteen by fifteen matrix to determine the fifteen "A" coefficients are presented here. These equations are extensions of the primary equations given in the text, namely, the neutron density equation, for slab 1

$$\frac{dn_1}{dt} = \frac{\delta K_1 n_1}{\ell} - \frac{K_1 \beta n_1}{\ell} + \sum_{i=1}^m \gamma_i \lambda_i C_{i1} + \frac{\alpha}{\ell} n_2(t - \tau) \quad (1c)$$

and the concentration equation for each of the six groups of delayed neutrons,

$$\frac{dC_{i1}}{dt} = \frac{K_1 \beta_i n_1}{\ell} - \lambda_i C_{i1} \quad (2c)$$

where subscript "i" refers to a specific delayed neutron group, thus, for six groups there are six equations of this form. Similarly for slab 2

$$\frac{dn_2}{dt} = \frac{\delta K_2 n_2}{\ell} - \frac{K_2 \beta n_2}{\ell} + \sum_{i=1}^m \gamma_i \lambda_i C_{i2} + \frac{\alpha}{\ell} n_1(t - \tau) \quad (3c)$$

$$\frac{dC_{i2}}{dt} = \frac{K_2 \beta_i n_2}{\ell} - \lambda_i C_{i2} \quad (4c)$$

As was done in the text, it is assumed that the solutions to these equations can be written

$$n_1 = \sum_{j=1}^{mm} A_{j1} e^{\omega_j t} \quad (5c)$$

$$n_2 = \sum_{j=1}^{mm} A_{j2} e^{\omega_j t} \quad (6c)$$

$$C_{11} = \sum_{j=1}^{mm} D_{1j1} e^{\omega_j t} \quad (7c)$$

$$C_{12} = \sum_{j=1}^{mm} D_{1j2} e^{\omega_j t} \quad (8c)$$

where A_{j1} , A_{j2} , D_{1j2} are constants determined by the initial boundary conditions. Subscript "j" refers to a specific root, and "1" or "2" refers to slabs number one or two.

The boundary conditions used in evaluating these constants are

$$\text{at } t = 0,$$

$$n_1 = n_{10} \quad (9c)$$

$$n_2 = n_{20} \quad (10c)$$

$$\frac{dC_{11}}{dt} = \frac{dC_{12}}{dt} = 0 \quad (11c)$$

$$(12c)$$

and for a rod drop into slab one, at $t = 0$,

$$\frac{dn_2}{dt} = 0. \quad (13c)$$

It is further assumed that initially the reactor is at steady state so that Equation 16 can be used to relate n_{10} and n_{20} as

$$n_{20} = - \frac{\alpha}{\delta k_2 n_{10}} \quad (14c)$$

Substitution of Equations 5C and 7C into Equation 2C and comparison of coefficients of the $e^{\omega_j t}$ terms yields the relationship

$$D_{1j1} = \frac{K_1 \beta_1 A_{j1}}{l(\omega_j + \lambda_1)} \quad (15C)$$

and similarly,

$$D_{1j2} = \frac{K_2 \beta_1 A_{j2}}{l(\omega_j + \lambda_1)} \quad (16C)$$

Substitution of Equations 6C and 16C into Equation 3C and again comparing coefficients of the $e^{\omega_j t}$ terms gives the relationship between the "A_j" coefficients in each slab.

$$A_{j2} = \frac{\alpha e^{-\omega_j \tau} A_{j1}}{\omega_j l - \delta K_2 + K_2 \sum_{i=1}^m \frac{\gamma_i \beta_i \omega_j}{\omega_j + \lambda_i}} \quad (17C)$$

When boundary condition 9C is applied to Equation 5C the result is the first of the fifteen required equations.

$$\sum_{j=1}^m A_{j1} = n_{10} \quad (18C)$$

Boundary condition 10C effects Equation 6C in a similar way.

This result is

$$\sum_{j=1}^m A_{j2} = n_{20} \quad (19C)$$

When expressed in terms of A_{j1} and n₁₀ this becomes

$$\sum_{j=1}^m \frac{\alpha e^{-\omega_j \tau} A_{j1}}{\omega_j l - \delta K_2 + K_2 \sum_{i=1}^m \frac{\gamma_i \beta_i \omega_j}{\omega_j + \lambda_i}} = - \frac{\alpha}{\delta K_2 n_{10}} \quad (20C)$$

which is the second required equation. Boundary condition 11C is applied to Equation 2C such that

$$\frac{dC_{11}}{dt} = \frac{K_1 \beta_1}{\ell} n_1 - \lambda_1 C_{11} = 0. \quad (21c)$$

Combining this expression with Equations 5C, 7C, and 18C, the result is a set of six required equations, one equation for each delayed neutron group.

$$\sum_{j=1}^{MM} \frac{A_{j1}}{(\omega_j + \lambda_1)} = \frac{n_{10}}{\lambda_1} \quad (22c - 27c)$$

These same relationships apply to the other slab such that

$$\sum_{j=1}^{MM} \frac{A_{j2}}{(\omega_j + \lambda_1)} = \frac{n_{20}}{\lambda_1}. \quad (28c - 33c)$$

Equations 28C - 33C are expressed in terms of A_{j1} and n_{10} through Equations 14C and 17C.

$$\sum_{j=1}^{MM} \frac{\alpha e^{-\omega_j \tau} A_{j1}}{\left(\omega_j \ell - \delta K_2 + K_2 \sum_{i=1}^{MM} \frac{\beta_i \omega_i}{\omega_j + \lambda_1} \right) (\omega_j + \lambda_1)} = \frac{-\alpha}{\lambda_1 \delta K_2 n_{10}} \quad (34c - 39c)$$

for a total of fourteen of the fifteen equations needed.

The fifteenth equation arises when boundary condition 13C is applied to Equation 6C, the result is

$$\frac{dn_2}{dt} - \sum_{j=1}^{MM} A_{j2} \omega_j e^{\omega_j t} = 0, \quad (40c)$$

which when expressed in terms of A_{j1} and n_{10} , becomes

$$\sum_{j=1}^m \frac{\alpha \omega_j e^{-\omega_j \tau} A_{j1}}{\omega_j l - \delta K_2 + K_2 \sum_{i=1}^m \frac{\gamma_i \beta_i \omega_j}{\omega_j + \lambda_i}} = 0 . \quad (41c)$$

These fifteen equations were solved for the " A_{j1} " coefficients by a digital computer program assuming n_{10} equal to unity. The resulting coefficients were then used in Equation 5C to determine the flux ratio in slab one after a rod drop. The " A_{j2} " coefficients were determined using Equation 17C and then used in Equation 6C to determine the flux ratio in slab two.

APPENDIX D

Miscellaneous Tables

Table 9. Delayed neutron half-lives, decay constants, relative abundances, and fission effectiveness for uranium-235

Group index i	Half-life seconds	Decay constant seconds ⁻¹	Relative abundance a ₁ /a	Fission effectiveness
1	54.51	0.0127	0.038	1.096
2	21.8	0.0317	0.213	1.028
3	6.00	0.115	0.188	1.050
4	2.23	0.311	0.407	1.033
5	0.496	1.40	0.128	1.000
6	0.179	3.87	0.026	1.000

Table 10. Flux decay in slab 2 after a rod drop into slab 1 of a two slab core reactor^a

Worth cents	Times after rod drop seconds						
	30	60	120	180	240	300	360
- 6.37	0.904	0.815	0.671	0.556	0.461	0.383	0.319
-12.74	0.768	0.639	0.453	0.325	0.235	0.170	0.123
-19.11	0.668	0.520	0.328	0.211	0.137	0.0895	0.0587
-25.48	0.591	0.437	0.251	0.148	0.0887	0.0537	0.0327
-31.85	0.531	0.375	0.200	0.110	0.0622	0.0356	0.0205
-38.22	0.483	0.329	0.165	0.0862	0.0464	0.0254	0.0141
-44.59	0.444	0.293	0.139	0.0700	0.0362	0.0192	0.0103
-50.96	0.411	0.265	0.121	0.0583	0.0294	0.0152	0.00797
-57.33	0.384	0.242	0.106	0.0499	0.0245	0.0124	0.00641
-63.70	0.360	0.223	0.0950	0.0435	0.0210	0.0105	0.00532

^a $\alpha = 0.010$, $\beta = 0.0065$, $\nu_{avg} = 1.034$, $\lambda = 0.0001$ seconds, $\tau = 2.10 \times 10^{-4}$ seconds.

Table 11. Flux decay in slab 1 after a rod drop into slab 1 of a two slab core reactor^a

Worth cents	Times after rod drop seconds						
	30	60	120	180	240	300	360
- 6.37	0.802	0.722	.595	0.493	0.409	0.340	0.282
-12.74	0.661	0.548	0.388	0.279	0.201	0.146	0.106
-19.11	0.557	0.433	0.272	0.175	0.114	0.0743	0.0487
-25.48	0.479	0.352	0.202	0.120	0.0713	0.0432	0.0294
-31.85	0.417	0.294	0.156	0.0859	0.0484	0.0277	0.0160
-38.22	0.369	0.250	0.125	0.0651	0.350	0.0192	0.0106
-44.59	0.330	0.217	0.103	0.0512	0.0265	0.0140	0.00754
-50.96	0.300	0.190	0.0861	0.0415	0.0209	0.0108	0.00565
-57.33	0.270	0.169	0.0737	0.0345	0.0169	0.00857	0.00442
-63.70	0.247	0.152	0.0641	0.0293	0.0141	0.00702	0.00356

^a $\alpha = 0.010$, $\beta = 0.0065$, $\gamma_{avg} = 1.034$, $\lambda = 0.0001$ seconds, $\tau = 2.10 \times 10^{-4}$ seconds.